THE CONSERVED OLIGOMERIC GOLGI (COG) COMPLEX IS REQUIRED FOR

NORMAL IMPORT OF FATTY ACIDS IN *SACCHAROMYCES CEREVISIAE*

APPROVED BY SUPERVISORY COMMITTEE

_____
Joel M. Goodman, Ph.D.

_____
Joseph P. Albanesi, Ph.D.

_____
Ronald A. Butow, Ph.D.

_____
Melanie H. Cobb, Ph.D.

To my loving wife, Karla

and

To my wonderful children, Morgan and Kristen

THE CONSERVED OLIGOMERIC GOLGI (COG) COMPLEX IS REQUIRED FOR

NORMAL IMPORT OF FATTY ACIDS IN *SACCHAROMYCES CEREVISIAE*


by


Johnathan L. Ballard


DISSERTATION


Presented to the Faculty of the Graduate School of Biomedical Sciences

The University of Texas Southwestern Medical Center at Dallas

In Partial Fulfillment of the Requirements

For the Degree of


DOCTOR OF PHILOSOPHY


The University of Texas Southwestern Medical Center at Dallas

Dallas, Texas

August, 2004

THE CONSERVED OLIGOMERIC GOLGI (COG) COMPLEX IS REQUIRED FOR

NORMAL IMPORT OF FATTY ACIDS IN *SACCHAROMYCES CEREVISIAE*

Johnathan L. Ballard, Ph.D.

The University of Texas Southwestern Medical Center at Dallas, 2004

Supervising Professor:  Joel M. Goodman, Ph.D.

The goal of my work was to elucidate aspects of the mechanism of trafficking of membrane proteins to peroxisomes. !The work described in this document centers around one protein from *Saccharomyces cerevisiae*, Cog7p. !Cog7p is part of the conserved oligomeric Golgi (COG) complex. !Results describing a basic function of Cog7p were published well after I began studying this protein. !Nevertheless, I use the nomenclature outlined in that work. !Cog7p functions in intra-Golgi vesicular transport in concert with seven other proteins. !This protein complex is found in both yeast and mammals. !We found Cog7p in a different context through a screen to identify proteins that function in the trafficking of membrane proteins to peroxisomes. !In the screen a portion of Cog7p was found to interact with the membrane peroxisomal targeting sequence, mPTS, of the *Candida boidinii* peroxisomal membrane protein, Pmp47. !I

studied peroxisomal biogenesis in a strain of *Saccharomyces cerevisiae* in which the *COG7* gene had been deleted. I showed that Cog7p was not required for peroxisomal biogenesis, but in so doing, established that Cog7p was required for the proper metabolism of fatty acids in a peroxisome-independent manner. I showed that Cog7p was required for the normal import of fatty acids; without Cog7p, yeast cells imported abnormally high amounts of free fatty acid from the environment. My results are consistent with the hypothesis that one or more protein(s) involved in fatty acid import require the COG complex for proper processing. My work ends before such a protein was identified, but I provide leads that if pursued would contribute to understanding the regulation of fatty acid import into yeast cells.

TABLE OF CONTENTS

(Page)

PUBLICATIONS

Wang X, McMahon MA, Shelton SN, Nampaisansuk M, Ballard JL, Goodman JM.

*Multiple targeting modules on peroxisomal proteins are not redundant: discrete functions*

*of targeting signals within Pmp47 and Pex8p.*  **Mol Biol Cell**. 2004 Apr;15(4):1702-10.

LIST OF FIGURES                                                    (page)

x

LIST OF TABLES                                                    (page)

# LIST OF ABBREVIATIONS

| | |
|---|---|
| AFA | activated fatty acid |
| Ade | adenine |
| AKL | alanyl-lysyl-leucine |
| ATP | adenosine triphosphate |
| BODIPY FL C12 | (4,4-difluoro-5,7-dimethyl-4-bora-3a,4a-diaza-s-indacene-3-dodecanoic acid) |
| BSA | bovine serum albumin |
| CoA | coenzyme A |
| COG | conserved oligomeric Golgi |
| COPI | coat protein complex I |
| COPII | coat protein complex II |
| DNA | deoxyribonucleic acid |
| ER | endoplasmic reticulum |
| EtBr | ethidium bromide |
| FFA | free fatty acid |
| GFP | green fluorescent protein |
| GST | glutathione S-transferase |
| His | histidine |
| HMS | Holland Minimal Salts |
| HMYD | Holland Minimal Medium Dextrose |

| | |
|---|---|
| HMYGO/L | Holland Minimal Medium Glycerol Oleate / Laurate |
| HMYO | Holland Minimal Medium Oleate |
| HMYO/L | Holland Minimal Medium Oleate / Laurate |
| HRP | Horse Radish Peroxidase |
| IgG | Immunoglobulin class G |
| LCFA | Long Chain Fatty Acid |
| MCFA | Medium Chain Fatty Acid |
| mPTS | membrane protein Peroxisomal Targeting Sequence |
| nha | sodium proton antiporter |
| ODU | Optical Density Unit |
| PCR | polymerase chain reaction |
| PBD | peroxisomal biogenesis disorder |
| PEX | peroxin |
| PMP | Peroxisomal Membrane Protein |
| PTS1 | Peroxisomal Targeting Sequence type 1 |
| SD | Synthetic Dextrose |
| SDS-PAGE | Sodium Dodecyl Sulfate-Polyacrylamide Gel Electrophoresis |
| Sec | Secretory mutant |
| SGd | Synthetic Glycerol dextrose |
| SNARE | soluble $N$-ethylmaleimide-sensitive-factor attachment protein receptor |

SPM                     Sporulation Medium

SR                      Synthetic Raffinose

t-SNARE                 target membrane- soluble *N*-ethylmaleimide-sensitive-

                        factor attachment protein receptor

URA                     Uracil

YPA                     Yeast extract Peptone Acetate

YPD                     Yeast extract Peptone Dextrose

YP                      Yeast extract Peptone

INTRODUCTION

*Overview of the secretory system*

Transit of proteins and lipids through the secretory system requires three steps: 1) budding of vesicles from donor membranes, 2) tethering/docking of vesicles to target membranes, and 3) fusion of vesicles to target membranes. To ensure proper localization of proteins traversing the system and of those residing in the organelles of the system, the specificity of these three steps must be tightly regulated. Proteins imparting specificity to the transport process have been identified at each step. Coat protein (COP) complexes regulate the budding process. Tethering factors provide long range associations between vesicle and target membranes, and the soluble N-ethylmaleimide-sensitive factor attachment protein receptor (SNARE) complexes are required for fusion events. They are located on target membranes (t-SNAREs) and on vesicles (v-SNAREs). Figure 1 depicts the organelles of the secretory/endocytic pathway and their relationships to several protein complexes involved in the transport of vesicles. Many proteins and lipids destined for various cellular locations are synthesized in the ER. Many of these molecules are modified with sugar moieties in the Golgi apparatus and subsequently sorted into appropriate vesicles for transport to their final destinations in the late Golgi. COPI operates in retrograde trafficking within the Golgi apparatus and from the Golgi to the ER. COPII is needed for ER-to-Golgi transport. The COG complex, exocyst, and GARP complex are related tethering complexes functioning at different steps in the secretory pathway. Sed5p is a Golgi t-SNARE. As depicted in figure 1, the Golgi apparatus, endosome, lysosome (vacuole), and

plasma membrane rely upon the ER for their lipid and protein components.  Recent work in elucidating mechanisms of peroxisomal biogenesis has provided compelling evidence that this is also the case for peroxisomes.

*Development of* Saccharomyces cerevisiae *as a model organism for studying the sorting of peroxisomal membrane proteins*

Peroxisomes are vital and versatile organelles (van den Bosch et al., 1992; Erdmann et al., 1997; Subramani 1998; Tabak et al., 1999; Smith and Schnell, 2001).  They are vital because defects in the function and biogenesis of these organelles cause inheritable and often fatal diseases in humans.  The lack of Pex19p disrupts the trafficking of matrix proteins and membrane proteins to peroxisomes causing Zellweger syndrome (Matsuzono et al., 1999).  Zellweger syndrome is one of several, heterogeneous diseases classified as peroxisomal biogenesis disorders (PBD).  These patients can exhibit severe hepatic, renal, and neurological dysfunction.  Variability in afflictions is owed to differing degrees to which peroxisomal biogenesis is disrupted.  In severe cases, like Zellweger syndrome where there are no peroxisomal remnants, the many metabolic pathways relying on compartmentalization of substrates and enzymes in the peroxisome no longer exist. Disruptions in peroxisomal function can impair the breakdown of fatty acids, the synthesis of bile acids, and the production of cholesterol in humans.  Peroxisomes are versatile as the number, size, and protein content of these organelles can change drastically to meet the metabolic needs of cells.  A case in point is the induction of peroxisomes in *S. cerevisiae* by oleic acid (Veenhuis et al., 1987).  Human disease states underscore the necessity of understanding the targeting of

peroxisomal membrane proteins (PMPs), and the induction of peroxisomes in *S. cerevisiae* provides the means to study this process in a genetically tractable system.

The nature of PMP targeting is open for debate. The controversy to resolve is whether PMPs are targeted directly to peroxisomal membranes or indirectly through another organelle. Evidence exists for both mechanisms. Pulse chase experiments with PMP70 showed that this protein was synthesized in the cytosol and transported directly to peroxisomes (Imanaka et al., 1996). Two peroxisomal proteins, Pex2p and Pex16p were glycosylated in the ER on their way to peroxisomes (Titorenko and Rachubinski, 1998). These two pathways are not mutually exclusive, and most models now incorporate both mechanisms (Erdmann et al, 1997; Sacksteder et al., 2000). In these models, the peroxisome is depicted as an extension of the ER in much the same way as are the Golgi and vacuole; peroxisomes require vesicle transport from the ER to supply proteins and lipids for their maturation. Geuze et al (2003) convincingly reconstructed by 3D electron microscopy a continuous network of membranous structures connecting the ER with peroxisomes through lamellae that contained both ER and peroxisomal proteins (figure 2). One striking feataure of their work was the lack of COPI and COPII coatamers in these membrane continuities. The nature of compartmentalization of the specialized ER and its maturation into peroxisomes may not require the budding and packing of traditional vesicles. The authors speculated that a dynamin-like pinching mechanism might be at work to separate preperoxisomes from the ER. PMP70 and Pex13p were localized to the preperoxisomal lamellae, but not the ER. The presence of PMP70 indicated that the lamellae were competent for importing PMPs from the cytosol. The question of whether the ER can is still

unanswered. PMPs that are required for the sorting of PMP70 could target via the ER, and one such candidate is Pex3p (Fang et al., 2004). Geuze et al (2003) proposed that Pex3p and perhaps Pex16p and Pex19p are targeted to the ER and trigger the formation of preperoxisomal lamellae. The targeting of Pex3p would be the initiating event as it serves as the docking site for the PMP receptor Pex19p (Fang et al., 2004), which in turn is involved in Pex16p targeting (Jones et al., 2004). A sought after goal, therefore, is to determine the exact mechanism for the trafficking of Pex3p, as this protein likely functions at an early stage in peroxisomal maturation. However, Pex3p and its associated import machinery may pull other PMPs into the ER before a transition to lamella or peroxisome is made. This may be the case for Pex16p, so evidence for the sorting of PMPs through the ER could come from the study of PMPs other than Pex3p.

The laboratory I joined in 1997 was focused on defining mechanisms of PMP targeting. The PMP used as a model for this process was Pmp47 from the yeast *Candida boidinii* (Goodman et al., 1986). A sorting system for this protein in *S. cerevisiae* was established ([b]McCammon et al., 1990), and the first targeting sequence for a peroxisomal membrane protein, termed an mPTS, was identified (McCammon et al., 1994; Dyer et al., 1996). Lastly, a two-hybrid screen was used to identify a protein that bound to the mPTS. This protein was Cog7p, and I joined the lab to determine if Cog7p was required for PMP sorting. The experimental approach chosen was to analyze PMP sorting in the absence of Cog7p. My loftiest aspiration for Cog7p was that it was responsible for the targeting of multiple PMPs. The absence of a protein involved in sorting several PMPs would cause gross abnormalities in peroxisome biogenesis and function because PMPs are required for

maintaining normal peroxisomal morphology (Hettema et al., 2000), importing peroxisomal matrix proteins (Girzalsky et al., 1999), and metabolizing fatty acids (Shani and Valle, 1996).

*β-oxidation in* S. cerevisiae

β-oxidation in *S. cerevisiae* takes place only in peroxisomes. The substrates for the first enzyme in the β-oxidation pathway, acyl-CoA oxidase, are fatty acids that have been activated to coenzyme A esters by acyl-CoA synthetases. Two pathways for activating fatty acids that are to be catabolized in peroxisomes exist in *S. cerevisiae* (figure 3). One of these pathways is specific for long chain fatty acids (LCFAs) such as (C18:1) oleic acid, and the other is specific for medium chain fatty acids (MCFAs) such as (C12:0) lauric acid.

*S. cerevisiae* can import free oleic acid (C18:1) from its surroundings and utilize it as a sole carbon source. Free oleic acid is activated to its coenzyme A ester by acyl-CoA synthetases. The oleoyl-CoA is then transported to peroxisomes where it enters the peroxisomal matrix via the Pxa1p/Pxa2p long chain acyl-CoA transporter (Hettema et al., 1996). The oleoyl-CoA is then catabolized into acetyl groups by the core enzymes of β-oxidation—Fox1p, Fox2p, and Fox3p—and a fourth enzyme, Eci1p, that is required to breakdown the double bond in the acyl chain (Gurvitz et al., 1999). The steps prior to import via Pxa1p / Pxa2p are poorly understood. The only proteins that have been shown to function in these steps are the acyl-CoA synthetases (Watkins et al., 1998) and Fat1p, which serves to present the fatty acids to the acyl-CoA synthetases (Zou et al., 2003).

*S. cerevisiae* can also utilize exogenously added lauric acid (C12:0) as a carbon source. Both oleic and lauric acids are catabolized by the same set of core β-

oxidation enzymes; however, the steps prior to the β-oxidation of MCFAs are significantly different from those prior to β-oxidation of LCFAs.  MCFAs enter peroxisomes as the free fatty acid species and are subsequently activated by Faa2p, a peroxisomal membrane associated acyl-CoA synthetase.  Two peroxisomal membrane proteins are required for MCFA catabolism—Pex11p (van Roermund, et al., 2000) and Ant1p (van Roermund et al., 2001).  Ant1p is a member of the mitochondrial solute carrier family of proteins.  This six-pass transmembrane domain protein is the *S. cerevisiae* homolog of *C. boidinii* Pmp47, which also functions in MCFA catabolism (Nakagawa et al., 2000). Both the knockout strain of *pex11* and the knockout strain of *ant1* have little medium chain acyl-CoA synthetase activity in intact cells but normal activity in cell lysates.   This suggests that these proteins function in presenting molecules necessary for the activation of MCFAs—possibly ATP and the MCFA themselves.  According to the literature cited above, these two pathways for transporting fatty acids into peroxisomes have overlapping specificities.  In mutants that lack one or both of the Pxa proteins, oleic acid is still catabolized, though at 20% of wild type levels, in a Faa2p dependent manner.  In a *pex11* knockout, MCFAs are catabolized at reduced levels in a Pxa2p dependent manner.


*Structure and function of the COG complex*

The conserved oligomeric Golgi (COG) complex is present in *S. cerevisiae*, *Drosophila* (Farkas et al., 2003), and mammals.  It is comprised of eight proteins, and it is found throughout the Golgi apparatus.  In *S. cerevisiae*, it is also called the Sec34/35 complex (Kim et al., 1999; VanRheenen et al., 1999), and in mammals it is also known as the

Golgi transport complex (GTC) and the ldlCp complex (Ungar et al., 2002). The complex

consists of eight proteins, and a few details about their organization within the complex are

known. The COG complex is localized to the Golgi apparatus and is required for the

retrograde transport of vesicles within that organelle. The function of the COG complex is

under investigation for two main reasons: 1) it is part of the exocyst family of complexes, so

it likely employs a mechanism that is utilized at multiple points in the secretory system and

2) it is required for the maintenance of the Golgi apparatus. The latter has implications for

human disease states.


**The *S. cerevisiae* COG complex**

The first two COG complex components identified in *S. cerevisiae* were

Sec35p and Sec34p (VanRheenen et al., 1998; 1999). [The COG designations, Cog2p and

Cog3p, respectively, were assigned later by Ungar et al., 2002, when it was shown that the

GTC and ldlCp complex were the same entity, and it was deemed necessary to have a

unifying nomenclature (Table I).] This initial identification came from a screen to identify

temperature sensitive mutations that block ER-to-Golgi transport. Both mutants at the

restrictive temperature accumulated numerous vesicles, which was indicative of defects in

the docking or fusion of transport vesicles. The authors devised an in vitro ER to Golgi

transport assay to reconstitute the activities of Cog2p and Cog3p. The assay followed the

modification of $\alpha$-factor with mannose to determine if the vesicle housing the protein was

delivered from the ER to the Golgi apparatus. When the assays were performed with

membranes prepared from wild type cells, the addition of the sugar moiety to $\alpha$-factor was

seen. No modification of α-factor was seen, though, when the assays were performed with membranes prepared without functional Cog2p or Cog3p. The membranes were prepared from the temperature sensitive mutants, and the assays were performed at the restrictive temperature. Modified α-factor was recovered upon the addition of purified wild type Cog2p or Cog3p to these reactions. These results indicated that these two Cog proteins were necessary for the docking or fusion of ER derived vesicles to the Golgi apparatus. Soon to follow, genetic and physical interactions between Cog2p and Cog3p were established (Kim et al., 1999; VanRheenen et al., 1999). Overexpression of Cog3p partially rescued the temperature sensitive allele of Cog2p, *sec35-1*, and the two temperature sensitive alleles of Cog2p and Cog3p, *sec35-1* and *sec34-2*, respectively, were synthetically lethal. Physical interactions between these two Cog components were seen with a two-hybrid assay and by co-immunoprecipitation experiments. Four additional, but unidentified, proteins were precipitated along with Cog2p and Cog3p suggesting they were two components of a larger complex. These two Cog proteins also eluted from gel filtration columns with an apparent size of >750 kD, much larger than a dimeric complex of each of these proteins.

Cog4p was the next component identified (Kim et al., 2001). The initial connection was made because Cog4p was a high-copy suppressor of the *cog2* mutation, *sec35-1*. The authors went on to show that Cog2p, Cog3p, and Cog4p co-immunoprecipitated and interacted in a two-hybrid system. *COG4* is an essential gene; therefore, a strain with *COG4* under the control of the galactose promoter was created to assess Cog4p's proposed role in the transport of vesicles. Reduced levels of Cog4p were achieved when this strain was grown on glucose. Upon the switch to glucose from galactose,

carboxypeptidase Y was delayed in traversing the secretory system, and multiple abnormalities with internal membranes were observed.  Similar abnormalities, such as accumulation a vesicles and dilated ER, were seen with the *sec34-2* and *sec35-1* strains. Additionally, this work reported the defective secretion of most proteins in these two mutants.  Cog3p was shown to colocalize predominantly with an early Golgi protein but also significantly with a late Golgi protein.

Cog8p was found to be synthetically lethal with Ric1p, a Golgi protein that functions in vesicle transport (Whyte and Munro, 2001).  They named this protein Dor1p, for dependent on Rci1p.  This work showed that Cog8p was part of a larger complex consisting of eight proteins.  Four of these were uncharacterized proteins, and they were given the Cod designation, for complexed with Dor1p.  Cog8p was tagged and precipitated from cellular lysates.  Coprecipitating proteins were identified according to the masses of their derived peptide fragments following tryptic digestion.  Three of these were the already known Cog components, Cog2p, Cog3p and Cog4p.  The other four were Cog1p, Cog5p, Cog6p, and Cog7p.  This was the first report of associations of Cogs 1, 5, 6, and 7 with the COG complex.  Even though these eight proteins were part of the same complex, their respective deletion strains showed differing phenotypes.  These phenotypic differences occurred in patterns leading Whyte and Munro (2001) to suggest a subclassification scheme for the COG complex.  Strains lacking the Cog proteins 1-4 were severely or totally defective for normal growth, while the remaining four, Cogs 5-8, were all nonessential genes.  Strains with mutations in *COG*s 1-4 displayed abnormalities with internal membranes and defects in Golgi processing of invertase.  These phenotypes were not seen with mutants in the other

group. All of the mutants in both groups, though, were defective in the recycling of the v-SNARE Snc1p. Based upon the differing phenotypes of the *cogΔ* strains, the hypothesis was proposed that the Cog complex was composed of two quartets, and quartet 5-8 was dispensable for some Cog complex functions.

Cog1p was independently identified from a temperature sensitive mutant, *sec36-1*, that was defective in the maturation of carboxypeptidase Y (CPY) (Ram et al., 2002). At the restrictive temperature, this mutant accumulated the ER modified form of CPY, which was consistent with a defect in the transport of vesicles from the ER to the Golgi apparatus. In agreement with the results of Whyte and Munro (2001) the *sec36-1* strain was also defective in invertase maturation, and it displayed severe defects in growth. Cog1p was present in immunoprecipitates of both Cog2p and Cog3p, and these three proteins comigrated upon gel filtration in a large complex of >800 kD. Cog3p was present in smaller complexes in the *sec36-1* (*cog1*) and *sec35-1* (*cog2*) strains, indicating that the structure of the COG complex was compromised in these mutants. The absence of Cog4p, Cog5p, Cog6p, Cog7p, or Cog8p also disrupted the elution of Cog3p during gel filtration. This was consistent with there being physical interactions among these eight proteins.

Most of the Cog components were identified through coprecipitation experiments. More than just the eight Cog proteins were brought down in such experiments (Suvorova et al., 2002). The most abundant proteins were purified and identified, but one group (Suvorova et al., 2002) identified more of these proteins by immunoblotting for proteins known to function in vesicular transport. In this way they achieved insight into the function of the COG complex. For instance, they identified the Golgi t-SNARE Sed5p and

α-COP1.  Several SNARE proteins with other cellular locations—including the ER, plasma membrane, and endosome— and COPII were not detected.  Genetic interactions were established between Cog3p and Sed5p and between the COPI complex and COG complex.  These results were consistent with the COG complex functioning in the retrograde transport of COPI-coated vesicles within the Golgi apparatus.  A disruption in retrograde transport could impair the recycling of components necessary for anterograde transport.  This, in turn, would disrupt secretion and ER-to-Golgi transport; therefore, the authors proposed that defects in anterograde transport seen in cells with COG complex deficiencies were secondary effects.

Two models (figure 4) were proposed for how the COG complex could function in retrograde transport (Suvorova et al., 2002).  The COG complex could act as a tethering factor for preformed vesicles, or it could help in the formation of retrograde vesicles by promoting the association of COPI with Golgi membranes.  The authors who proposed the model favored the former scenario because it took into account the function of small GTPases (see below) and the accumulation of small vesicles in some *cog* mutants.  Bruinsma, et al (2004) though, favored the latter model.  They predicted *sed5* mutants and *cog3* mutants would sort the Golgi mannosyltransferase Och1p to the same retrograde vesicle if these two mutants disrupted the same tethering/fusion event.  Since Och1p localization differed in these mutants, the authors argued that Och1p was stuck in retrograde vesicles in the *sed5* mutant, while Och1p was never loaded into these vesicles in the *cog3* mutant and wound up in an unidentified post-Golgi compartment.  As Bruinsma et al (2004) noted, the

tethering and loading models are not mutually exclusive; the COG complex may perform both functions.

**The mammalian COG complex**

The above observations from *S. cerevisiae* were complemented by studies on the mammalian COG complex (Ungar et al., 2002). These reports established that, like its yeast counterpart, the mammalian COG complex consisted of eight components that were localized to the Golgi compartment. Data were also presented that this complex was required for normal Golgi operation.

It was determined that human Cog3p localized with the cis/medial Golgi marker membrin under normal conditions and after Nocodazole treatment, which fragmented the Golgi apparatus (Suvorova et al., 2001). In this study Cog3p migrated as a 300 kD species on glycerol velocity gradients consistent with its existence in a multiprotein complex. In another report on mammalian Cog3p (Loh and Hong, 2002), antibodies reacting specifically with Cog3p inhibited an in vitro transport assay measuring the ER-to-Golgi transport of vesicular stomatitis virus envelope protein (VSVG). Cog3p was localized with the Golgi SNARE GS28, and Cogs 1, 2, 4, 5, 6, and 8 were found in immunoprecipitates of Cog3p. As stated above, the COG nomenclature was established by Ungar et al., 2002. In this report, all eight mammalian COG components were identified from a Cog5p containing complex purified from bovine brain cytosol, and immunoprecipitations confirmed physical associations among Cogs 1, 2, 3, and 5. Deep etch EM showed that the COG complex likely had a bilobed architecture, which is consistent with the subclassification scheme proposed by

Whyte and Munro (2001). Work presented in Loh and Hong (2004) provides further support for the bilobed structure while making predictions about the assembly process of the complex. Using Cog proteins expressed from in vitro translation systems, all the necessary combinations of immunoprecipitations were performed to characterize the interactions among the eight COG complex components. Seven binary interactions were detected for six of the components: Cog1/3, Cog1/4, Cog2/3, Cog2/4, Cog4/5, Cog4/7, and Cog5/7. Cog6p interacted with the Cog5/7 complex, and Cog8 interacted with a ternary Cog5/6/7 complex. From these sets of interactions a model describing the assembly of the COG complex was proposed (figure 5). The model depicts a bilobed structure connected by Cog4p. A relationship with COPI was also established for the mammalian COG complex (Oka, et al., 2004). The intracellular distributions of ε-COP, a COPI component, and Cog1p were dependent upon each other. The distributions of a particular set of resident Golgi proteins called GEARS were also dependent upon ε-COPI and Cog1p. As mentioned above, studies with the *S. cerevisiae* COG complex resulted in two models of how this complex might function in the transport of vesicles. These two models may well represent two halves of the general mechanism of vesicle transport. A report by Morsomme and Riezman (2002) showed that Cogs 2 and 3 were required for the loading of GPI-anchored proteins into discreet vesicles at the ER. They proposed a model in which protein complexes form on donor membranes that contain elements required for the loading/budding from the donor membranes and elements required for future tethering/docking at target membranes.

**The quatrefoil family of tethering complexes**

The COG complex, the exocyst (Sec6/8 complex in mammals), and the Golgi-associated retrograde protein (GARP) complex (Conibear et al., 2003) [also known as the VFT (Vps fifty three) complex in yeast] comprise the quatrefoil family of tethering complexes (Short and Barr, 2002; Whyte and Munro, 2002).  The exocyst is required for the transport of late-Golgi derived vesicles to the plasma membrane.  The GARP complex is required for the transport of endosome-derived vesicles to the Golgi apparatus.  These complexes are called quatrefoil tethering complexes to denote their function while eluding to the fact that the number of proteins in each complex is a multiple of four (Whyte and Munro, 2002).  The exocyst and COG complex are each comprised of eight proteins, and the GARP complex has four components (Table II).  Whyte and Munro (2001) were the first to recognize sequence similarities among members of these complexes.  They reported similarities between the following pairs:  Cog8p/Sec5p, Cog3p/Exo70, and Sec3p/Vps52p (Table II).  It is hoped that the quatrefoil complexes are enough alike that information gathered about one complex will apply to the other member complexes.  Recent work into quatrefoil complex interactions with small GTPases and t-SNAREs shows that this situation is being realized.  The proper localization of the exocyst component Sec3p in yeast requires two Rho GTPases, Rho1p and Cdc42p.  Another exocyst component Sec15p binds preferentially to the GTP-bound form of the Rab GTPase Sec4p, which is present on secretory vesicles.  The interaction of the GARP complex with Ypt6p Rab GTPase is required for its localization to late Golgi membranes. Suvorova et al (2002) reasoned that the COG complex would interact with a small GTPase.  Their candidate was the Rab GTPase

Ypt1p because overexpression of Ypt1p suppresses temperature sensivitive mutations of *sec34* and *sec35* (vanRheenen et at., 1998; 1999). The found that purified COG complex preferentially bound the GTP form of GST-Ypt1p. Purified Cog2p and Cog3p did not bind to Ypt1p, suggesting that other COG complex components were responsible for the interaction. As described above the yeast COG complex interacts with the Golgi t-SNARE Sed5p. The strategy to define the site of action of the COG complex by identifying the t-SNARE with which it interacts was reasonable given that the exocyst binds to the plasma membrane t-SNARE syntaxin (Hsu et al., 1996). Information gained about the COG complex will have implications not just for a specific function at a specific cellular location in a specific organism but for a specific function at multiple cellular locations in all eukaryotes.

### *COG7* deficiency underlies a human disease state.

The importance of studying the COG complex is underscored by discovery that a *cog7* deficiency has severe consequences for humans. Wu et al., 2004, report the case of two siblings who died 5 to 10 weeks after birth. Both had severe liver dysfunction and epilepsy. They suffered from recurrent infections and cardiac insufficiency. Isoelectric focusing of the serum protein transferrin glycoconjugates from the siblings revealed an abnormal pattern. Fibroblasts from one of the siblings had defects in both N- and O-linked glycosylation, which signaled severe defects in Golgi function. The activity of ST3Gal-I, a resident Golgi glycosyltransferase, was reduced to 62% of normal levels, and the trafficking of this protein into the Golgi apparatus was retarded. These characteristics were reminiscent

of COG mutants in CHO cells, so the locations of the COG proteins, except Cog4p, in fibroblasts of the siblings were analyzed by indirect immunofluorescence. Cogs 1,2, and 3 localized with a Golgi marker, whereas, Cogs 5,6, and 8 were cytoplasmic. There was no detectable Cog7p staining in these cells, suggesting that the absence of Cog7p could be the underlying defect in these patients. Both patients had identical point mutations in both copies of their *COG7* genes. Reintroduction of the *COG7* gene into these patients' fibroblasts rescued the defects in glycosylation and trafficking. It also restored the Golgi localization of Cog5p; Cog6p and Cog8p localization were not determined. From the model proposed by Loh and Hong (2004) an absence of Cog7p would prevent the binding of Cog6p and Cog8p to lobe B. Their model allows for the binding of Cog5p to lobe A under these circumstances, but Cog5p did not localize with lobe A in the siblings fibroblasts. The binary interaction between Cog4p and Cog5p seen by Loh and Hong may not be sufficient for in vivo association. The siblings had a congenital disorder of glycosylation (CDG). Prior to this report, the causes of CDG were defects in enzymes or transporters directly involved in glycosylation reactions. The glycosylation defects in the CDG patients with *cog7-*deficiencies were indirect consequences of more global defects in Golgi function that affected the maturation of the enzymes responsible for the glycosylation reactions. These findings defined a new category of CDG.

The experiments described next summarize my work on the characterization of a *cog7* deficiency in *S. cerevisiae*. Study into the function of Cog7p began with emphasis on its proposed role in the sorting of membrane proteins to peroxisomes. PMPs still targeted to peroxisomes without Cog7p, but the *cog7Δ* strain

imports large amounts of extracellular fatty acid.  The identities of all of the proteins affected by the loss of the COG complex, or more specifically, by the loss of lobe B are unknown.  Likewise, as will be discussed in the conclusion, all of the components that control the import of fatty acids are unknown.  The *cog7Δ* strain constitutes a system with which the relationship between vesicular transport and the import of fatty acids can be explored.  The opportunity exists to refine the role of the COG complex in secretion while discovering new aspects of the regulation of the import of fatty acids.
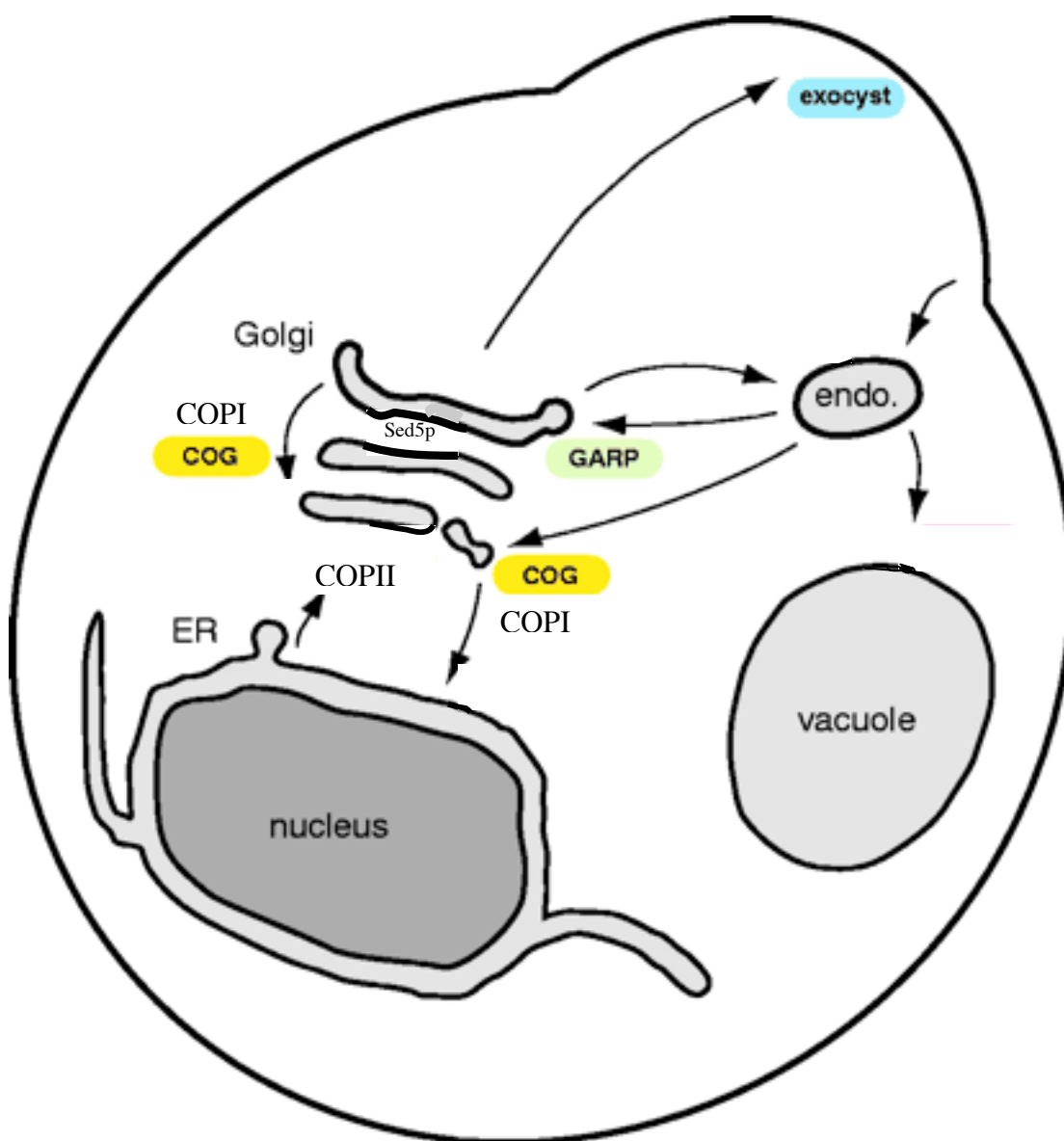
*Adapted from Whyte and Munro, 2002

Figure 1          Overview of the secretory/endocytic pathway in yeast.

Shown are the organelles along the pathway and several protein complexes at their sites of action.  COPI operates in retrograde trafficking within the Golgi apparatus and from the Golgi to the ER.  COPII is needed for ER-to-Golgi transport.  The COG complex, exocyst, and GARP complex are related tethering complexes functioning at different steps in the secretory pathway.  Sed5p is a Golgi t-SNARE.
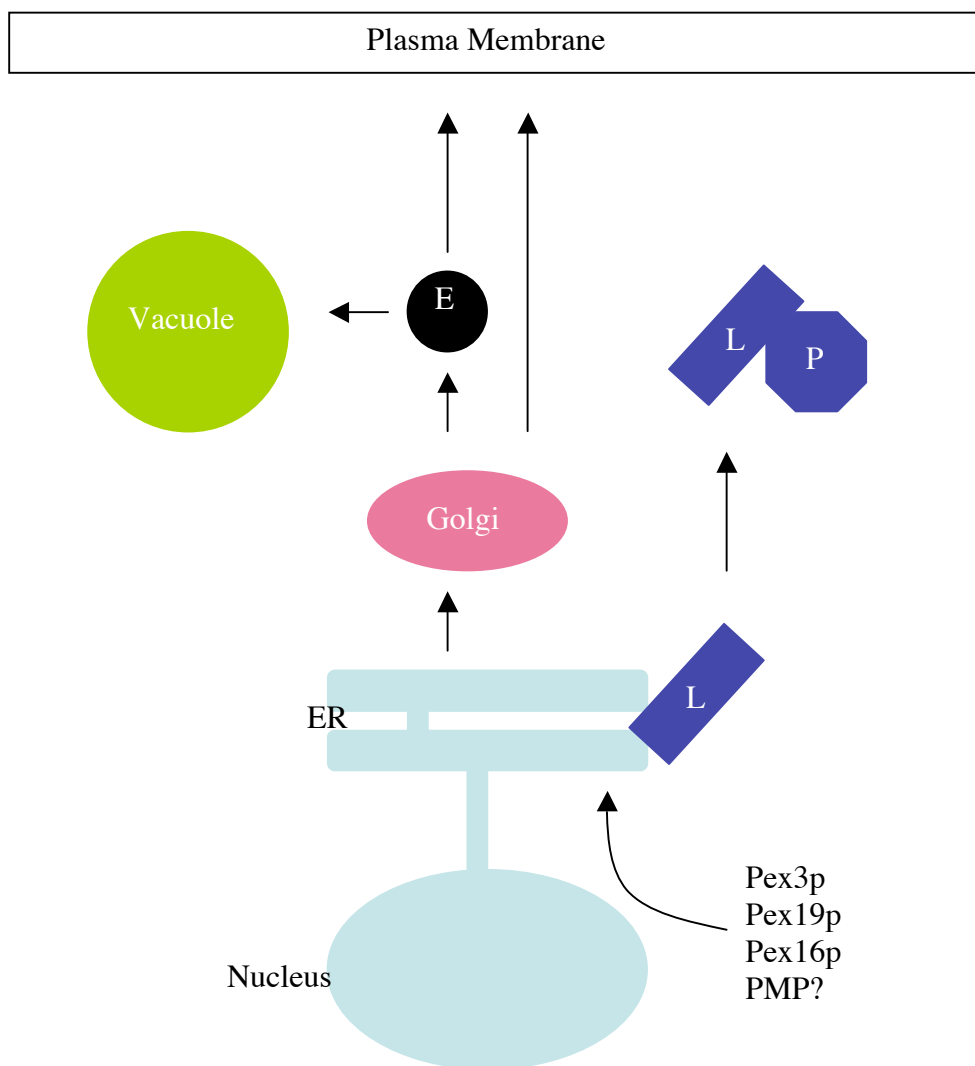
*Adapted from Tabak et al., 2003

Figure 2          The ER-to-Peroxisome Maturation Pathway

The insertion of PMPs into the ER, possibly Pex3p and Pex16p, initiate the formation of the preperoxisomal lamellae.  Eventually the lamellae become competent for matrix protein import and evolve into mature peroxisomes.  E = endosome, ER = endoplasmic reticulum, L = lamellae,  P = peroxisome
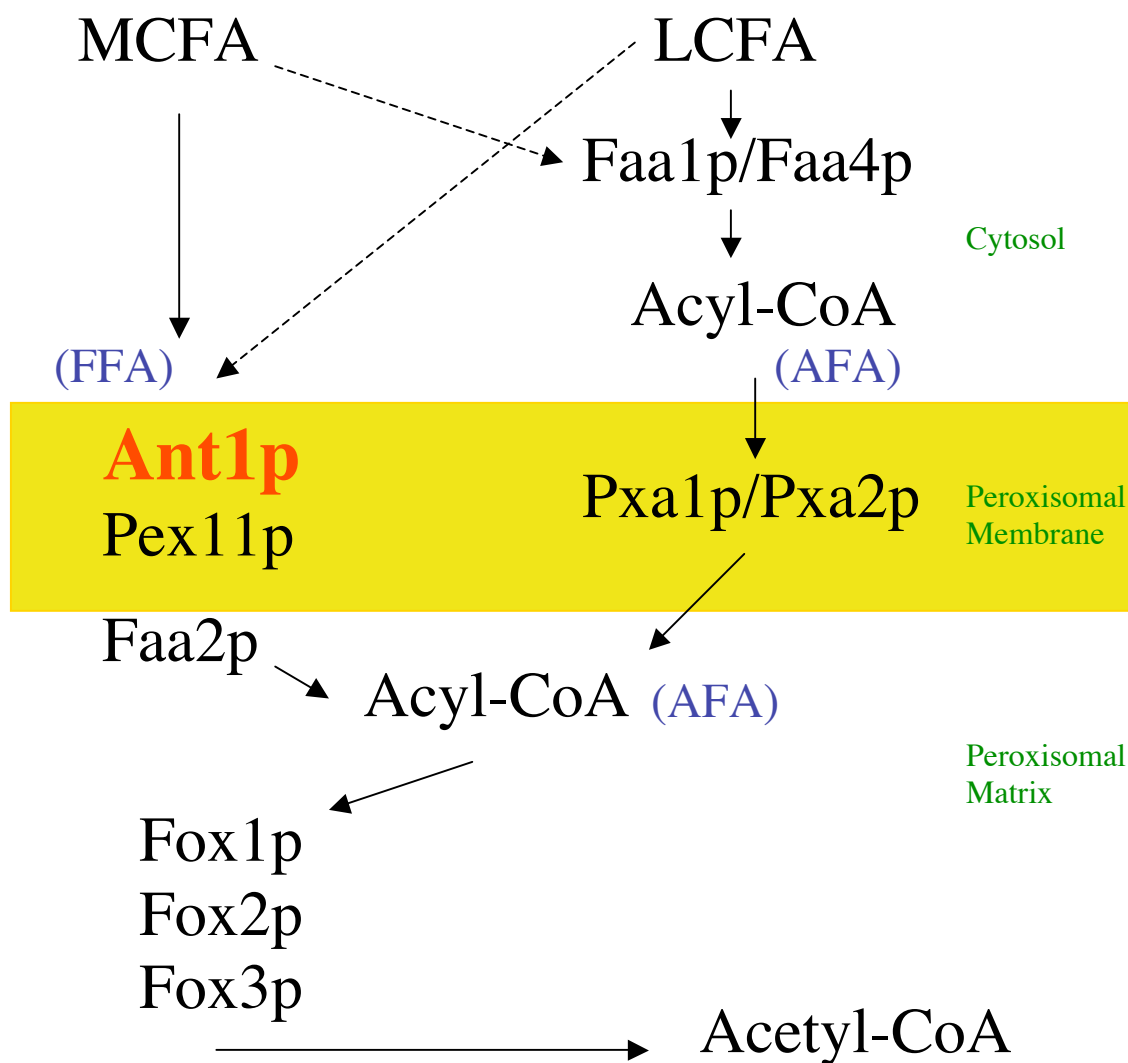
Figure 3          β-oxidation in *S. cerevisiae*

The two pathways of β-oxidation are shown.  Solid arrows denote the flow of fatty acids across the peroxisomal membrane, and the proteins involved in their breakdown to acetyl-CoA are listed.  Overlap between the pathways is denoted by dashed arrows.  AFA = activated fatty acid, FFA = free fatty acid, LCFA = long chain fatty acid, MCFA = medium chain fatty acid

TableI

NOMENCLATURE OF THE COG COMPLEX SUBUNITS

| Subunit | Previous Mammalian Nomenclature | Previous *S. cerevisiae* Nomenclature |
|---------|-------------------------------|------------------------------------|
| Cog1 | ldlBp | Cod3p/Sec36p |
| Cog2 | ldlCp | Sec35p |
| Cog3 | hSec34p | Sec34p/Grd20p |
| Cog4 | hCod1p | Cod1p/Sgf1p/Sec38p |
| Cog5 | GTC-90 | Cod4p |
| Cog6 | hCod2p | Cod2p/Sec37p |
| Cog7 | None | Cod5p |
| Cog8 | hDor1p | Dor1p |

Adapted from Ungar et al., 2002

**A** Tethering

COPI

RETROGRADE
TRANSPORT
VESICLE

SEC34/35P
COMPLEX

V-SNARE

GTP-
YPT1P

T-SNARE

CIS-GOLGI

**B**
Cargo sorting

SEC34/35P
COMPLEX

COPI
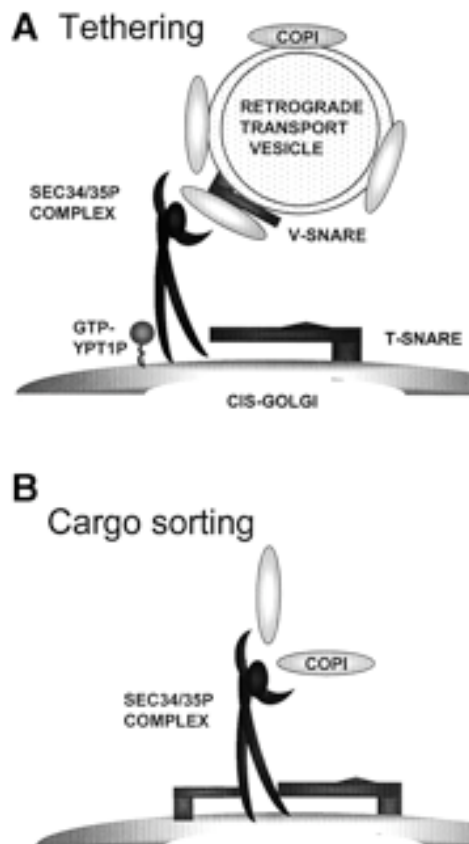
*Adapted from Suvorova et al., 2002

Figure 4        Two models of how the COG complex might function in vesicular transport.

The COG complex could act as a tethering factor for preformed vesicles, or it could help in the formation of retrograde vesicles by promoting the association of COPI with Golgi membranes to initiate cargo sorting.

Lobe B                                   Lobe A
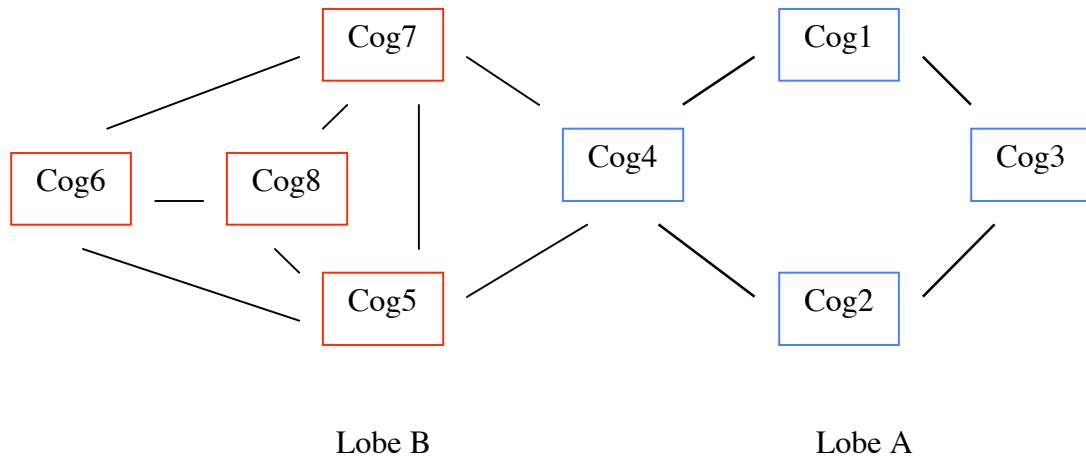
*Adapted from Loh and Hong, 2004

Figure 5          Model for the assembly of the Cog complex

Seven binary interactions were detected for six of the components: Cog1/3, Cog1/4, Cog2/3, Cog2/4, Cog4/5, Cog4/7, and Cog5/7.  Cog6p interacted with the Cog5/7 complex, and Cog8p interacted with a ternary Cog5/6/7 complex. The model depicts a bilobed structure connected by Cog4p.

Table II

## QUATREFOIL TETHERING COMPLEXES

| Exocyst | COG complex | GARP complex |
|---------|-------------|--------------|
| Sec3*** | Cog1 | Vps51 |
| Sec5* | Cog2 | Vps52*** |
| Sec6 | Cog3** | Vps53 |
| Sec8 | Cog4 | Vps54 |
| Sec10 | Cog5 | |
| Sec15 | Cog6 | |
| Exo70** | Cog7 | |
| Exo84 | Cog8* | |

*,**,*** having sequence similarities according to Whyte and Munro, 2001.

MATERIALS AND METHODS

*Strains*

Two *Escherichia coli* strains were used. BL21 cells (Studier and Moffatt, 1986) were used for the expression of a GST-Cog7p fusion protein. TG-1 cells (Gibson, 1984) were used for the amplification of plasmids.

Three strains of *S. cerevisiae* were used in this study. The diploid strain MMYODIP1 (Marshall et al., 1995) was used to test if *COG7* was essential. A heterozygous *cog7Δ* strain was made by gene replacement and confirmed by PCR and Southern analysis. Sporulation of the heterozygous strain was achieved by growth on YPA to log phase followed by several days culturing in SPM. Tetrad analysis was done with standard microdissection techniques. All other experiments were performed with haploid strains in one of the following two genetic backgrounds: MMYO11α ([a]McCammon et al., 1990) and BY4742 (ResGen Invitrogen Corporation). All mutants in the BY4742 background were purchased from Invitrogen. The cog7D, pex19D, and pxa2D mutants in MMYO11α were created by gene replacement. The pex11D derivative was created by gene disruption (Marshall et al., 1995). The ρ° derivatives were created according to (Fox et al., 1991). Briefly cells were passaged twice in liquid YPD-EtBr and recovered on YPD plates. Clone 10 (MMYO11α *ade-2-1::URA3 GFP-AKL*) is a derivative that contains a genomic integration of green fluorescent protein fused to a PTS1. A cog7D derivative was made in clone 10 by gene replacement. Spontaneous Ade[+] revertants of clone 10 and clone

10::cog7D were obtained be culturing on SD minus adenine. All strains depicted in figures are from the MMYO11α background, unless otherwise stated.

*Media and culturing*

The media used are the following: 10X YP (10% yeast extract, 20% peptone); YPD (1% yeast extract, 2% peptone, and 2% dextrose); YPD-EtBr (YPD plus 25 ug/mL ethidium bromide); YPA (1% yeast extract, 2% peptone, 2% potassium acetate); SPM (0.3% potassium acetate, 0.02% raffinose); SGd (3% glycerol, 0.1% dextrose, 0.67% Yeast Nitrogen Base [Difco] plus appropriate amino acids to satisfy auxotrophic requirements); SD (2% dextrose, 0.67% Yeast Nitrogen Base plus amino acids); SR (2% raffinose, 0.67% Yeast Nitrogen Base plus amino acids); HMS (pH6, 0.25% $(NH_4)_2SO_4$, 0.02% $MgSO_4$ $7H_2O$, 0.3% $NaH_2PO_4$ H2O, and 0.07% $K_2HPO_4$); HMYO (a semisynthetic medium containing 0.1% oleic acid [McCammon et al., 1990]); HMYO/L (a semisynthetic medium containing 0.07% oleic acid and 0.03% lauric acid); HMYGO/L (HMYO/L plus 3% glycerol). The oleic/lauric acid mixture was made by heating 0.5 mL of oleic acid with 250 mg of lauric acid at 70º C for 20 min with frequent vortexing. The resulting liquid was added to a final concentration of 0.1% to the semisynthetic medium (HMY).

For growth in fatty acid medium, cells are grown for 48 hours in SGd and boosted for four hours after the addition of 1/10$^{th}$ the culture volume of 10X YP. The cells are then spun out of YP and suspended at 1 $OD_{600}$ in fatty acid medium. There were two exceptions: 1) the immunogold labeling experiment for thiolase and 2) whole cell lipid analysis depicted in figure 17. For these experiments, cells were grown in semisynthetic

medium with 2% glucose (HMYD) until they were doubling every three hours.  They were then diluted 1:5 into HMYO for peroxisomal induction.  All culturing, unless otherwise specified, was done at 30ºC.  Growth was monitored using optical density (OD) readings at 600 nm.

*Reagents*

Lipid standards were purchased from Sigma (178-4).  Fatty acid free bovine serum albumin (BSA) was purchased from Sigma (A-6003).  BODIPY FL C12 (4,4-difluoro-5,7-dimethyl-4-bora-3a,4a-diaza-s-indacene-3-dodecanoic acid) was purchased from Molecular Probes (D-3822).  Pyranine was purchased from Molecular Probes (H-348).  Lauric acid was purchased from Aldrich (15378-8).  Oleic acid was purchased from Aldrich (26,804-6).  Oleic acid [1-$^{14}$C] was purchased from NEN.  D-glucose-6-$^{3}$H(N) was purchased from Sigma (G3399).  DNA-modifying enzymes were purchased from New England Biolabs.

*Plasmids*

The *COG7* open reading frame was inserted downstream of glutathione S-transferase (GST) using the pGEX-1 system (Smith and Johnson, 1988).  The plasmid, pPmp47-(1-267)-GFP, is used to express a fusion protein consisting of the first 267 amino acids of *C. boidinii* Pmp47 linked to GFP in *S. cerevisiae* (Wang et al., 2001).   The plasmid, pRS315-11/47A is used to express full-length *Candida boidinii* Pmp47 in *S. cerevisiae* under control of the oleate inducible *PEX11* promoter.  The plasmid, pComp, contains a *S.*

*cerevisiae* genomic DNA fragment containing the *COG7* promoter, open reading frame, and

terminator cloned into the BamHI and SacI sites of pRS314 (Sikorski and Hieter, 1989). The

genomic fragment was obtained by PCR with the primers 5'

CGCGGATCCGATTGCTGGTCACGTTTCTGG 3' and 5'

AGCGAGCTCATCATGGCGATCATTGGCAGC 3'. This plasmid was used to

complement the *cog7Δ* strain. The plasmid pRS314 was used for mock complementations.

The plasmid pRS424-11COG7 was generated to over-express Cog7p in *S. cerevisiae*. The

*COG7* open reading frame was put under the control of the *PEX11* promoter in the 2μ

plasmid pRS424 (Sikorski and Hieter, 1989). A *S. cerevisiae* genomic DNA fragment

generated from the following PCR primers—5'

CCGGAATTCATGGTAGAGTTGACAATTACG 3' and

5'AAACTGCAGATCTGAAATAGCATGTCCTCC 3'—was ligated into the EcoRI and PstI

sites of pKS-24-5'3' (Dyer et al., 1996). The KpnI and BamHI fragment of the resulting

plasmid was cloned into pRS424.


*Immunoblotting*

SDS-PAGE (Laemmli, 1970) was performed with 9% acrylamide and a

separating gel at pH 9.2. Immunoblots were performed with Enhanced Chemiluminescence

reagents (Amersham Life Science). Anti-mouse IgG, goat, HRP conjugated was purchased

from BioSource (AM10404). Anti-rabbit IgG, sheep, HRP conjugated was purchased from

Cappel (55677). The polyclonal anti-Sec61p was a kind gift from Randy Sheckman. The

antibody against Pmp47 is described elsewhere (Goodman et al., 1986). The antibody

against Pex11p is described elsewhere (Marshall et al., 1995). The antibody against porin was purchased from Molecular Probes (A-6449). The αCog7p antibody was raised in rabbits against a GST-Cog7p fusion protein.

*Whole cell lipid analysis*

Lipids were extracted from whole cells after growth on fatty acid medium. Equal optical density units of cells for each strain were extracted in 2-propanol and chloroform. The organic phase was washed several times with 1M KCl. Lipids were separated by thin layer chromatography on Si gel G 250 μm layer, analytical glass plates. The solvent was hexane: diethyl ether: acetic acid (80:20:1). Lipids were visualized with iodine vapor. Lipid standards were chromatographed for comparison purposes.

*Measuring β-oxidation*

Cells were grown in HMYGO/L to induce peroxisomes. For repression of peroxisomes, cultures were grown in YPD. Two and a half optical density units (2.5 ODU 600nm) were harvested and washed twice in HMS before suspension in 1mL of HMS to give a final concentration of 2.5 ODU/mL. Reactions were set up in 25mL Kontes flasks with septums and center wells as follows: 200 μL of cells, 800 μL HMS, 1 mL of 20 μM $^{14}$C oleic acid in HMS. The center wells contained filter paper soaked in 200 μL of 2M NaOH. The reactions were incubated for 0, 15, 30, or 60 minutes at 30ºC. The reactions were killed with the addition of 1 mL 3M $H_2SO_4$, and the $CO_2$ was collected for 1 hour. Radioactivity in the

filter paper was quantified by scintillation counting.  Cell counts were determined from colony counts on YPD plates.

*Fatty acid import assays*

**Cellular association of ¹⁴C oleic acid**.

Wild type and *cog7Δ* cells were harvested in log phase from YPD cultures for these assays.  Aliquots of cells were incubated with 10 μM ¹⁴C oleic acid for 0 and 2 minutes. Fatty acid free bovine serum albumin was added to a final concentration of 25 μM to stop the reactions, and the cells were spun down and washed to remove any label not associated with the cells.  The amount of cell-associated label was quantified by scintillation counting, and rates for the two minute periods were calculated as pmol/min/1x10^8 cells.  Cells were counted with a hemacytometer.

**Cellular association of ³H glucose.**

Wild type and *cog7Δ* cells were grown to log phase in YPD, starved for 5 hours, and treated with 200 nM ³H-glucose.  Aliquots of cells were filtered and washed at 0, 30, 60, and 90 seconds.  The cell-associated (filter-associated) radioactivity was quantified by scintillation counting.  Controls for non-specific binding of glucose to the filters were used, and these background counts were subtracted from counts generated when cells were present.  Cell counts were determined with a hemacytometer.

**Import of BODIPY FL C12.**

The import assays were performed according to Faergeman et al., 1997, with minor changes.  All culturing was done on YPD.  Cells were harvested and then were washed with and suspended in HMS.  Cells were treated with 10μM BODIPY FL C12, washed with HMS, and viewed with confocal laser scanning microscopy.  Treatment times, BSA exposure, and the presence of oleic acid varied among experiments.  Specifics are given in the figure legends.

*Other methods*

Fluorescence and indirect immunofluorescence of *S. cerevisiae* was performed as described in Wang et al., 2001.  Electron microscopy was performed as described in Marshall et al., 1995.  Whole cell lysates from yeast were prepared by glass bead lysis, and protein concentrations were determined with amido black (Schaffner and Weismann, 1973).  Yeast cells were transformed with the lithium acetate method (Ito et al., 1983).  Standard recombinant DNA techniques were performed (Sambrook, 1989). Organellar fractionations and extractions were done as described in Marshall et al., 1995. Briefly, cells are subjected to osmotic lysis and differential centrifugation is used to obtain an organellar pellet (25,000 x g pellet).  This pellet is subjected to separation on Nycodenz gradients or to extraction with 0.1M sodium carbonate, $Na_2CO_3$.  Proteins in the samples are analyzed by SDS-PAGE, staining, and immunoblotting. The pHi was determined with the fluorescent dye, pyranine, according to the protocol of Pena et al., 1995, after cells had grown in SGd for 48 hours.

RESULTS

*Creation of the* cog7Δ *strain*

The experimental approach chosen to determine if Cog7p was required for

PMP sorting was to analyze the process in the absence of Cog7p.  This approach required a

*S. cerevisiae* strain lacking Cog7p.  I created a haploid *cog7Δ* strain by targeted gene

replacement.  If a null mutation is lethal, it is possible by this procedure to isolate a strain

with the desired knockout that owes its viability to a second site mutation.  Such a situation

would confound the analysis of the mutant strain.   To address this concern, I created a

heterozygous *cog7Δ* diploid strain and assessed spore viability.  If a null mutation is viable,

then a heterozygous mutant should produce four viable spores.  If it is lethal then the lethality

and viability should segregate in a 2:2 pattern.  A *cog7* deletion is not lethal, as all four

spores from a single cell were viable, but a 2:2 pattern of slow growth at 37ºC was evident

(figure 1A).  The presence of the *HIS3* gene coincided with the heat sensitive growth

retardation, suggesting that this phenotype was caused by the *cog7* deletion.

I took advantage of this phenotype to confirm that the haploid *cog7Δ* strain

created initially was correct.  This strain also exhibited the growth defect (figure 1B & C),

and growth was restored by reintroduction of *COG7* (figure 1D).  Further confirmation that

the strain was correct, and that I could proceed with the PMP sorting analysis, was obtained

from immunoblots for Cog7p (figure 2).   By blotting equal amounts of protein from whole

cell lysates of wild type, *cog7Δ*, *cog7Δ* complemented, and Cog7p over-expresser strains, I

was able to confirm the absence of Cog7p in the null strain and the presence of wild type
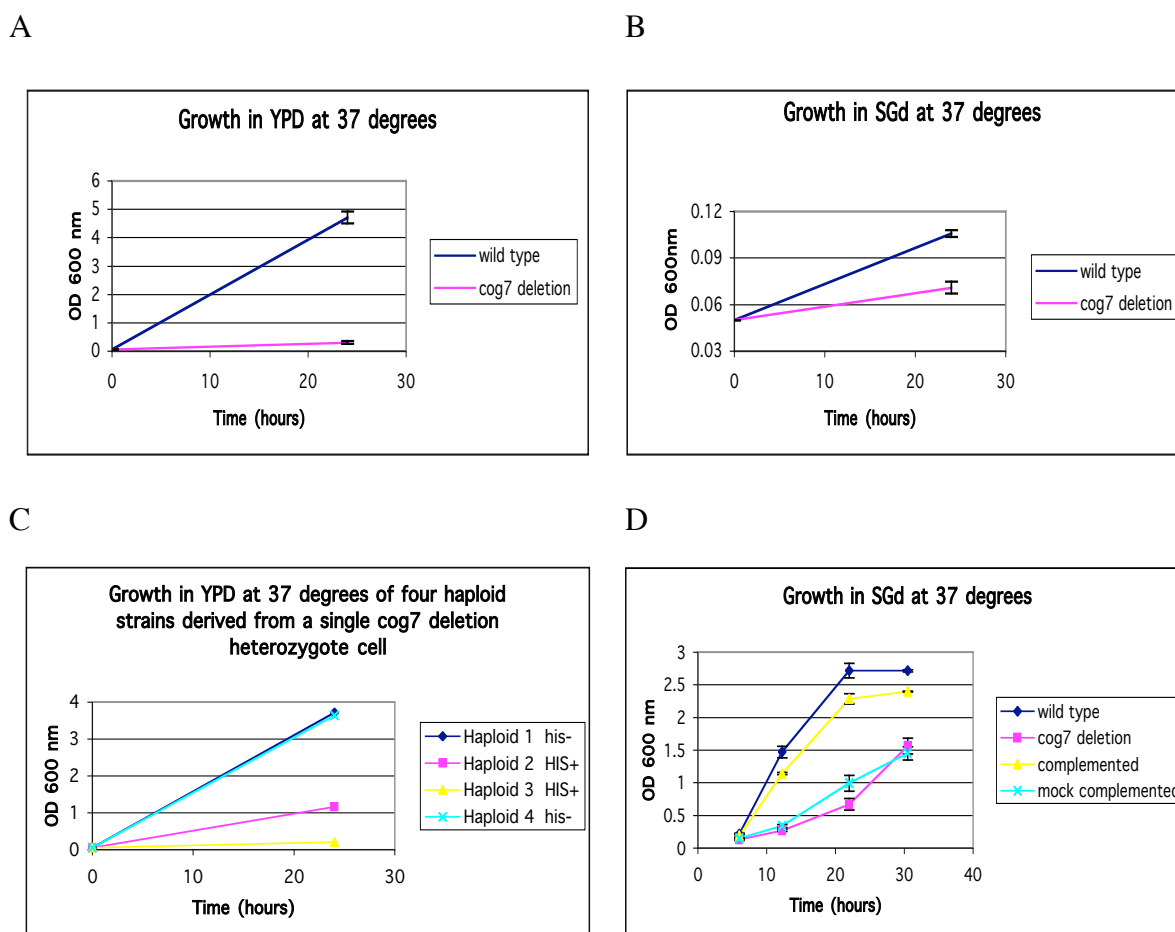
levels in the complemented strain.

Figure 6    The *cog7Δ* strain exhibited a temperature sensitive growth defect at 37°C.

Cultures of wild type and *cog7Δ* were inoculated in 15 mL YPD (**A**) or 15 mL SGd (**B**) at an optical density at 600nm (OD$_{600}$) of 0.05 and allowed to grow at 37°C for 24 hours. The OD$_{600}$ of the cultures at 24 hours were determined and plotted as the average of three independent cultures ± standard deviation. The wild type strain reached much higher OD$_{600}$ than did the *cog7Δ* strain. The difference in growth was more pronounced in rich media (YPD). (**C**) Strains derived from the four spores of a single heterozygous *cog7Δ* diploid cell were assayed as in A. The two histidine[+] strains are *cog7Δ*, and the two histidine[-] strains are wild type. The His[+] strains grew poorly compared to the His[-] strains. (**D**) The following strains were cultured as in B, but multiple time points were taken over a 30 hour period: wild type, *cog7Δ*, *cog7Δ* transformed with pComp, and *cog7Δ* transformed with pRS314. Time points are the average of three independent cultures ± standard deviation. The complemented *cog7Δ* strain grew like the wild type strain. The mock complemented strain grew more slowly like the *cog7Δ* strain.
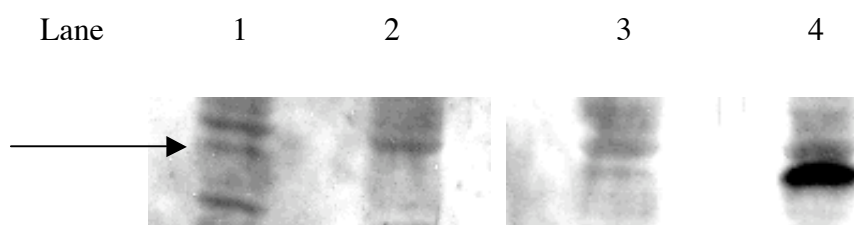
Figure 7    Immunoblots for Cog7p confirmed the genotypes of the *cog7Δ* and *cog7Δ* complemented strains.

Thirty micrograms of protein from whole cell lysates of oleic acid grown wild type, *cog7Δ*, *cog7Δ* transformed with pComp, and *cog7Δ* transformed with pRS424-11COG7 (lanes 1,2,3, & 4, respectively) were separated by SDS-PAGE, transferred to nitrocellulose, and blotted for Cog7p.  The arrow denotes the Cog7p band.  The blots show the absence of Cog7p in the *cog7Δ* strain, the wild type levels in the complemented strain, and the above wild type levels in the Cog7p over-expresser strain.

*Pmp47 function and sorting in the* cog7Δ *strain*

   I chose to analyze peroxisome morphology, matrix composition, and function in the *cog7Δ* strain to look for gross abnormalities in peroxisomal biogenesis.  It was quite possible, however, that Cog7p was required for the sorting of only a small number of PMPs and the effects of its absence on peroxisomes as a whole would be minimal.  Just as likely was the possibility that Cog7p played no role in the trafficking of PMPs; the interaction between Cog7p and the mPTS seen in the two-hybrid assay could be non-physiological or could reflect a function unrelated to the sorting of PMPs.  For these reasons, studies that specifically addressed the sorting and function of Pmp47 were embedded in those experiments designed to look for gross abnormalities in peroxisomal biogenesis.

**Pmp47 functioned normally in the *cog7Δ* strain.**

   A disturbance in peroxisomal biogenesis will cause a reduction in the rate of β-oxidation, which manifests as impaired growth on fatty acid medium.  If Cog7p functions in the targeting of PMPs, then the *cog7Δ* strain should grow poorly on oleic acid medium.  At the very least, only if Pmp47 sorting is affected, growth on oleic acid should be retarded in *cog7Δ* because of the partial catabolism of oleic acid through the MCFA pathway.

   When grown on glucose / glycerol medium at 30°C the *cog7Δ* strain has a slight growth defect that is complemented by reintroduction of *COG7* (figure 3).  Severely impaired growth, however, is seen when the *cog7Δ* strain is cultured in oleic acid (figure 4).  The *cog7Δ* strain grows slightly better than wild type cells in medium with no carbon source

and slightly better than *pex19Δ* cells, which have a total disruption of peroxisomal biogenesis (Gotte et al., 1998). Again, this defect is complemented by reintroduction of *COG7*. These results indicate that peroxisomal biogenesis may be compromised in *cog7Δ*.

If Cog7p is required for the sorting of only Pmp47, one expects similar growth characteristics for *cog7Δ* and *ant1Δ* strains on fatty acid medium. The comparison of these two mutants was performed in a different background strain of *S. cerevisiae*, BY4742, because these mutants were readily available along with the *cog8Δ* strain. This strain was included to link these phenotypes with the absence of the COG complex. The growth of BY4742 is poor on oleic acid medium, making it nearly impossible to discern retardation in growth from wild type levels. Better growth is seen, though, when the strain is cultured on a mixture of oleic and lauric acids (figure 5). Figure 6 shows that BY4742 and the three mutants all grow equally well in glucose / glycerol medium before the switch to the oleic / lauric acids medium where the growth patterns diverge. Growth in this mixed medium was entirely dependent upon Ant1p. The two *cogΔ* strains had similar phenotypes that were distinct from the *ant1Δ* phenotype. The two *cogΔ* strains grew better than the *ant1Δ*, suggesting that Ant1p is active in these strains if only partially. If the COG complex plays any role in Pmp47 sorting it will be a minor one.

The *cogΔ* strains exhibit the requisite growth defect on fatty acid media. The next step was to determine if a reduction in β-oxidation was the cause. Defects in other areas of lipid metabolism can cause growth defects on fatty acid medium (Faergeman et al., 1997), so to establish a link to peroxisomal biogenesis, a reduction in β-oxidation must be observed in these strains.

As a measure of β-oxidation, the conversion of $^{14}C$ oleic acid to $^{14}C$ $CO_2$ was compared between the wild type and *cog7Δ* strains.  The wild type strain grown on glycerol/fatty acid medium ("wild type induced") was used as a positive control for the assay, and wild type cells grown on glucose ("wild type repressed") served as a negative control, as the synthesis of β-oxidation enzymes is repressed in the presence of glucose. Figure 7 shows that the rate of β-oxidation for induced wild type cells is much greater than for repressed wild type cells.  In addition, the β-oxidation of oleic acid was measured in *pex11Δ* and *pxa2Δ* cells, which are defective in the medium chain fatty acid β-oxidation pathway and the long chain fatty acid β-oxidation pathway, respectively.  Oleic acid is broken down in part by both pathways, so these are additional controls for the experiment. Figure 7 shows that each pathway accounts for approximately half of the oleic acid β-oxidation activity.  No difference in activity could be detected for the *cog7Δ* strain.  Since the wild type level of β-oxidation of oleic acid requires a functional MCFA pathway and the *cog7Δ* strain exhibited wild type levels, Ant1p must function correctly in this strain.  Since Ant1p likely transports ATP through the peroxisomal membrane for the activation of MCFAs within the peroxisome (van Roermund et al., 2001), it is unlikely that Pmp47 can function if mistargeted.  These results indicate that Cog7p does not function in the sorting of Pmp47. This idea is supported by results presented in the next section.
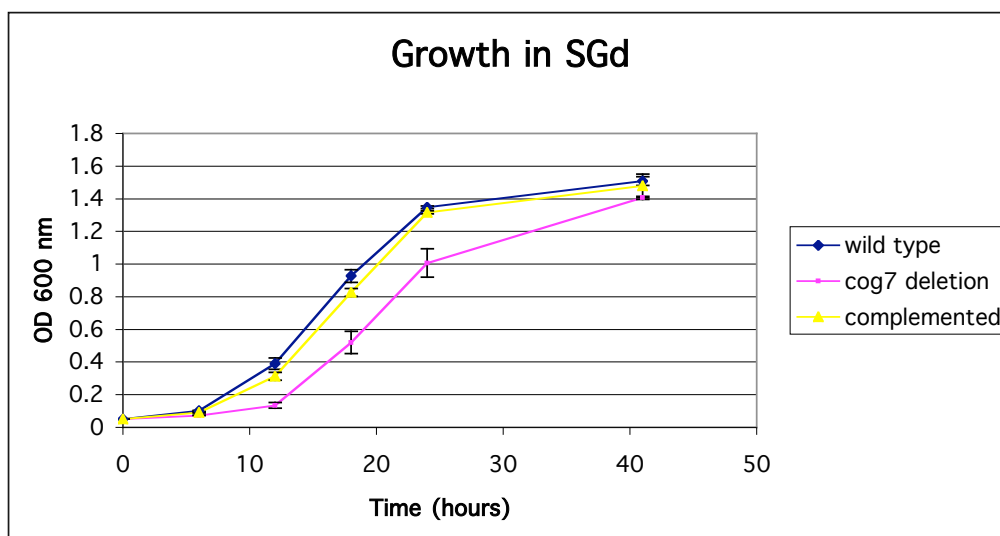
Figure 8       The *cog7Δ* strain exhibited nearly normal growth on synthetic glycerol dextrose medium.

Wild type, *cog7Δ*, and *cog7Δ* complemented strains were inoculated into SGd at 0.05 $OD_{600}$. The $OD_{600}$ of each culture was taken at various time points for two days. The time points represent the average of three independent cultures ± standard deviation. There was a slight growth defect for the *cog7Δ* strain that was absent in the complemented *cog7Δ* strain.
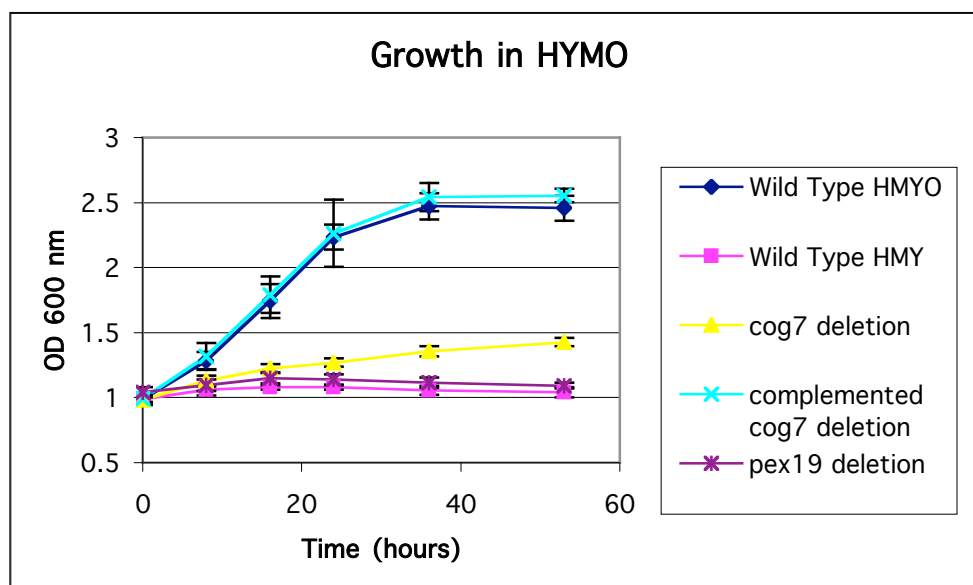
Figure 9     Cog7p was required for optimal growth on oleic acid medium.

Wild type, *pex19Δ, cog7Δ*, and the complemented *cog7Δ* strains were grown in SGd medium before suspending each in HMYO at 1 OD$_{600}$.  Oleic acid cultures were 40 mL in 250 mL flasks.  Wild type cells were also cultured without oleic acid in the medium (in HMY).  The optical densities were taken at various time points for approximately three days.  Each time point represents the average of at least four independent cultures ± standard deviation.  Wild type and complemented strains grew well, while the wild type no carbon source and *pex19Δ* strains did not grow.  The *cog7Δ* strain grew poorly.
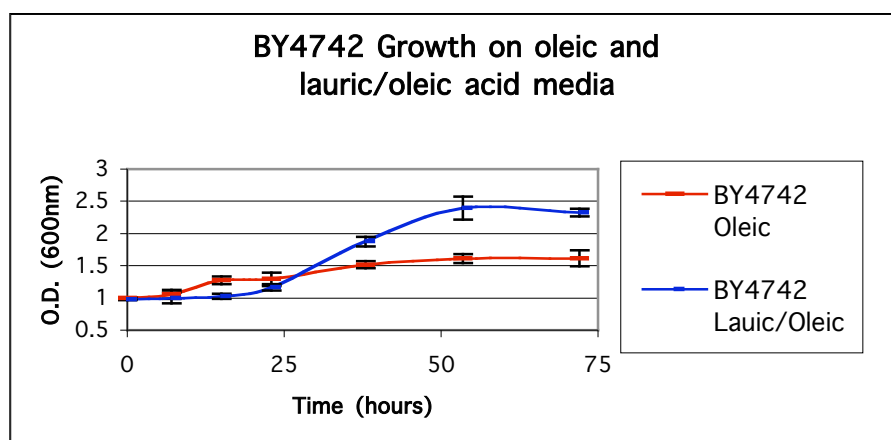
Figure 10    BY4742 grew better on HMYO/L than on HMYO.

The growth curves are done in the indicated medium with the strains listed in the legend. Preculturing was done as described in Materials and Methods. The BY4742 strain was then grown in either HMYO or HMYO/L for approximately three days. . The optical densities were taken at various time points for approximately three days. Each time point is the average± standard deviation of at least three independent cultures. Fatty acid culture volumes were 40mL in 250 mL flasks. The BY4742 grew better on the mixture of oleic and lauric acids.

A



B
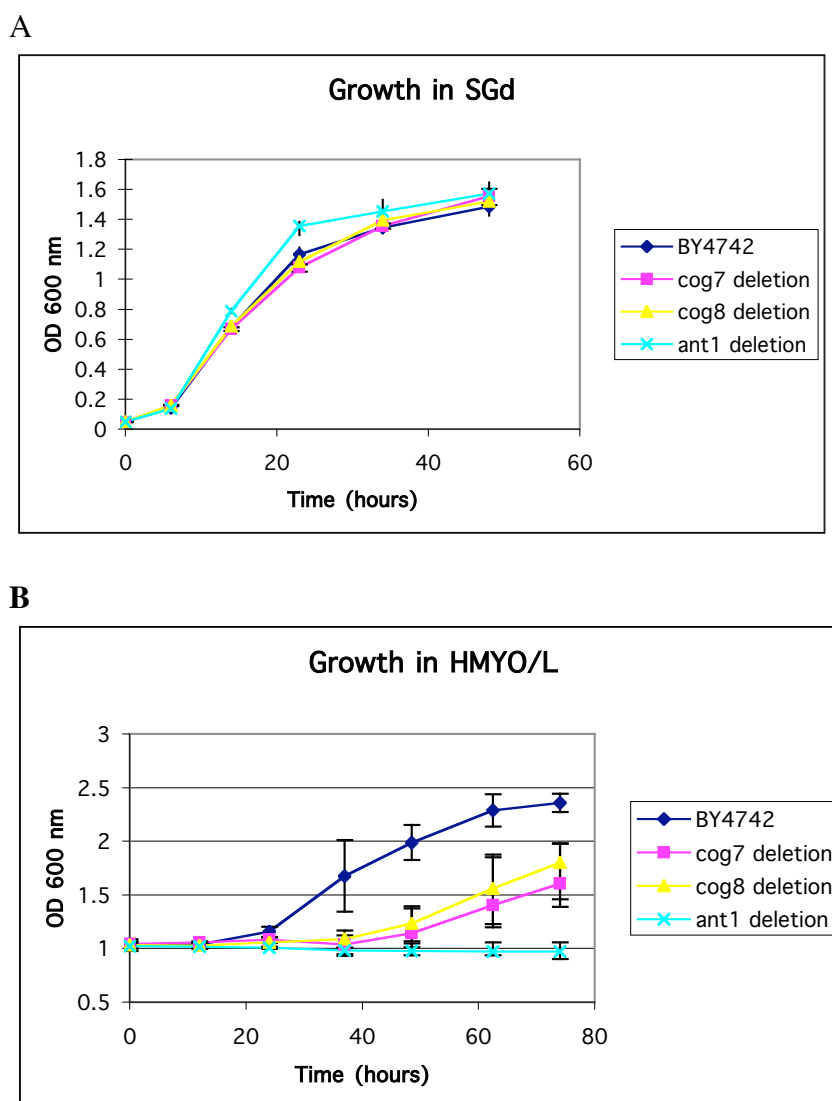


Figure 11     Cog7p and Cog8p were required for optimal growth on fatty acid medium.

**(A)** The growth patterns of the BY4742, BY4742*::ant1Δ,* BY4742*::cog7Δ,* and BY4742*::cog8Δ* were followed for two days on synthetic glycerol dextrose (SGd) medium. Cultures were inoculated to an $OD_{600}$ of 0.05, and the $OD_{600}$ was determined at various time points. All strains grew equally well with dextrose and glycerol as carbon sources. **(B)** After 48 hours in SGd, the strains were suspended in HMYO/L. They were suspended to an $OD_{600}$ of 1.0, and the $OD_{600}$ was taken at various time points for three days. The fatty acid cultures were 40 mL contained in a 250 mL flask. BY4742 grew well compared the *ant1Δ*, which is defective for the MCFA pathway. The *cog7Δ* and *cog8Δ* strains grew poorly compared to BY4742. All culturing was done at 30ºC, and time points are the average of four individual cultures per strain ± the range.

**beta-oxidaton of oleic acid**

Legend:
- Wild Type induced
- cog7 deletion
- pex11 deletion
- pxa2 deletion
- Wild Type repressed
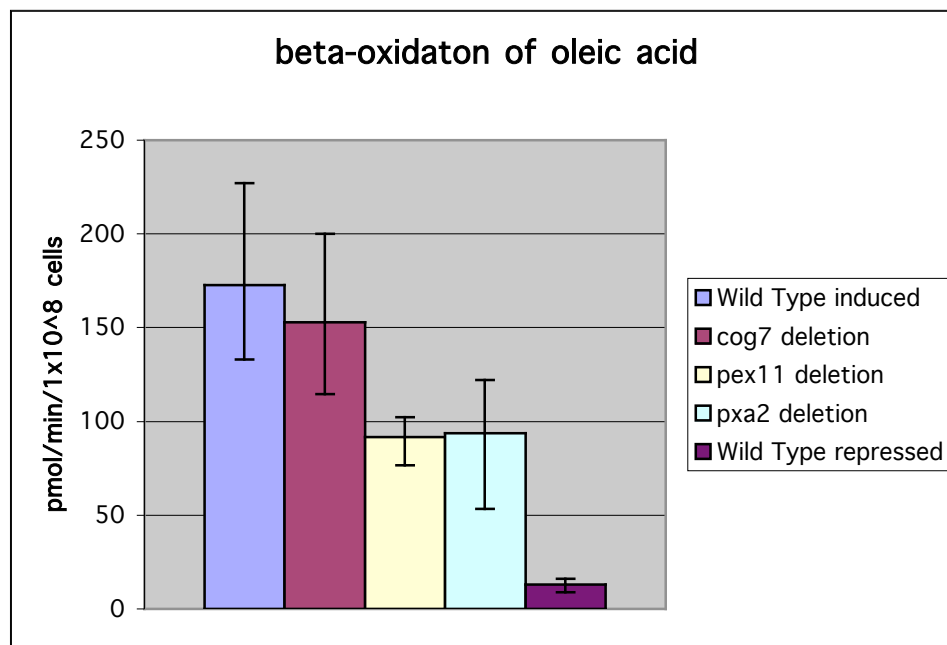
Figure 12    The β-oxidation of oleic acid was normal in the *cog7Δ* strain.

Wild type, *cog7Δ, pex11Δ,* and *pxa2Δ* cells were grown to saturation in SGd medium.  The strains were then inoculated into HMYGO/L.  The strains were grown until log phase (~20 hours for wild type and *pxa2Δ* and 43 hours for *cod5Δ* and *pex11Δ)* and then harvested for whole cell measurements of β-oxidation upon exposure to 10 μM $^{14}$C-oleic acid.  As a negative control, β-oxidation was measured for wild type cells harvested from log phase glucose grown cultures ("wild type repressed").  The rate of β-oxidation was determined by quantifying the amount of $CO_2$ produced over a 60-minute period using 0, 15, 30, and 60 minute reactions.  The rates were linear during the 60-minute period.  The rates are expressed as pmol/minute/1x10^8 cells.  Shown are the averages from three independent cultures +/- the range of the values.  Cell counts were determined from colony counts on YPD plates.

**Pmp47 localized to peroxisomes in the *cog7Δ* strain**.

Peroxisomes can be purified and separated from other organelles based on differences in organellar density. Since defects in peroxisomal biogenesis can alter the protein components of peroxisomes and thus their density (Dyer et al., 1996), I chose to purify peroxisomes for the *cog7Δ* strain to look for any deviations. In addition, the purification procedure allows me to follow individual peroxisomal proteins so the fate of Pmp47 in the *cog7Δ* strain can be determined. Will Pmp47 colocalize with peroxisomal marker proteins?

The purification experiments were designed to test whether the targeting and insertion of Pmp47 was defective in the *cog7Δ* strain. *Candida boidinii PMP47* under the control of the oleic acid inducible *PEX11* promoter was introduced into the *cog7Δ* strain. The colocalization of Pmp47 with peroxisomal markers upon peroxisomal purification and the extraction of Pmp47 from membranes with sodium carbonate were evaluated. Unfortunately, immunoblots for mitochondrial porin and Pex11p on the Nycodenz gradient fractions for *cog7Δ* revealed that mitochondria and peroxisomes could not be separated from one another (figure 8). The non-separation of organelles from the *cog7Δ* strain rendered this technique inadequate for evaluating Pmp47 targeting to peroxisomes. Peroxisomes from the *cog7Δ* strain have aberrant densities, but the deviations are not specific to peroxisomes. Evaluation of the extraction of Pmp47 from organellar pellet membranes revealed that it was more extractable by sodium carbonate in the *cog7Δ* strain than in the wild type strain (figure 9). Figure 10 shows that, like the abnormal organellar densities, this extraction phenotype is

not limited to peroxisomes. An ER membrane protein and a mitochondrial membrane protein are also more easily extracted from their respective membranes.

An in vivo approach was needed for the colocalization studies since purification of organelles from the *cog7Δ* strain was problematic. Studies with a fluorescent peroxisomal matrix protein indicated that the *cog7Δ* strain had distinct peroxisomes present in normal numbers. Electron microscopy confirmed this while justifying the use of the peroxisomal matrix protein, thiolase, in fluorescence-based colocalization studies with Pmp47.

Given the comigration of organelles on density gradients, I needed to know if distinct peroxisomes even existed in the *cog7Δ* strain. I had to establish the nature of peroxisomes in the *cog7Δ* strain in order to set up colocalization experiments with Pmp47. Green fluorescent protein (GFP) targets to peroxisomes in *S. cerevisiae* when fused to a type 1 peroxisomal targeting sequence, or PTS1 (Dyer et al., 1996). This fusion protein, GFP-AKL, fluorescently labels the peroxisomal matrix. Figure 11 shows that *cog7Δ* cells that express GFP-AKL have a punctate fluorescence pattern similar to that of the wild type strain. If these structures represent distinct peroxisomes, then they exist in wild type numbers (figure 12).

The ultimate proof that normal peroxisomes are present in the *cog7Δ* strain came from electron micrographs. Peroxisomes are darkly stained organelles bound by single membranes. Such organelles are clearly present and distinct from mitochondria in the *cog7Δ* strain (figure 13). The interiors of these structures were labeled with antibodies to the peroxisomal matrix protein thiolase (figure 14). The micrographs also display a phenotype

seen in approximately ten percent of the *cog7Δ* cells, the massive proliferation of the ER

(figure 15).

Since distinct peroxisomes exist in *cog7Δ* cells, colocalization studies were

performed with Pmp47 and thiolase.   A Pmp47-GFP fusion protein (Wang et al., 2001) was

colocalized with thiolase using direct fluorescence and indirect immunofluorescence,

respectively (figure 16).  Pmp47 can target to peroxisomes in the *cog7Δ* strain.

I was looking for a protein that functioned in the targeting of Pmp47 and

perhaps other PMPs to peroxisomes.  I reasoned that lack of such a protein would disrupt

peroxisome biogenesis and function.  At the very least, disrupting β-oxidation of medium

chain fatty acids.  The data presented above suggest that Pmp47 targets to peroxisomes and

that the *S. cerevisiae* homolog, Ant1p, functions properly in the absence of Cog7p.  I

conclude that Cog7p does not have a role in sorting Pmp47 to peroxisomal membranes.
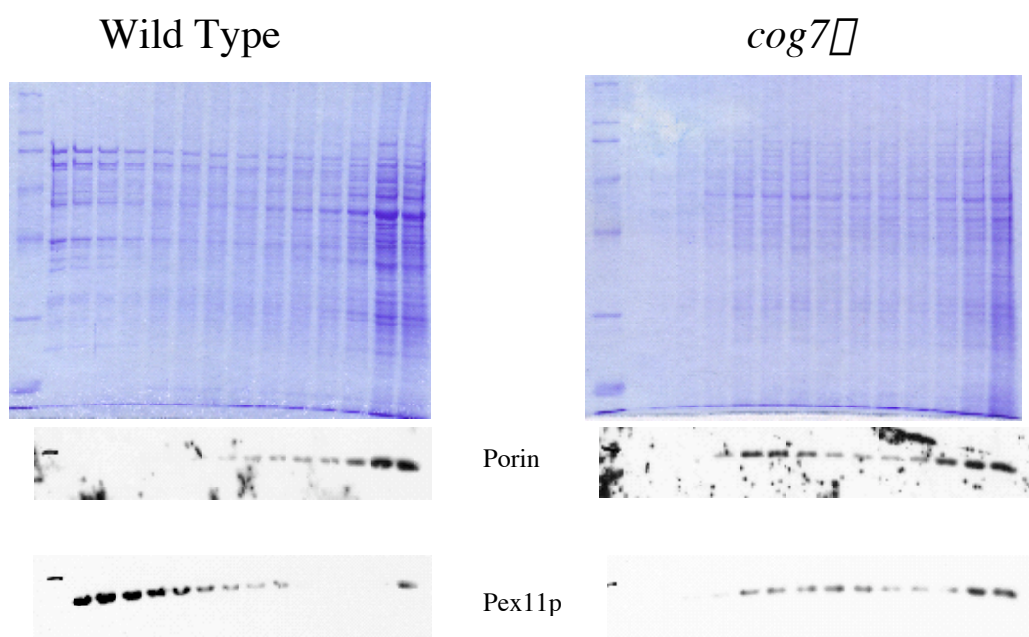
Figure 13    The organellar migration on Nycodenz density gradients was altered in the *cog7Δ* strain.

Wild type and *cog7Δ* strains were grown in SGd medium before suspending each in HMYO at 1 $OD_{600}$. After overnight incubation at 30°C, organellar (25,000xg) pellets were prepared for separation on Nycodenz gradients. Each Nycodenz density gradient was divided into14 fractions of equal volume. Equal volumes of each fraction were run on SDS-PAGE gels to separate proteins. Density increases from left to right. The left most lanes are protein molecular weight standards. The gels were stained by Coomassie blue to visualize the proteins. Immunoblots of the same gradient material for porin and Pex11p showed the migration of mitochondria and peroxisomes, respectively. Both organelles migrated aberrantly in the *cog7Δ* strain.
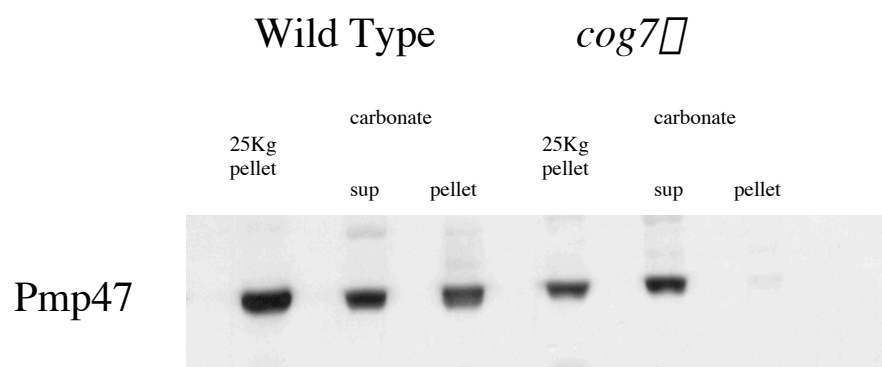
Figure 14     Heterologously expressed *Candida boidinii* Pmp47 was more extractable with sodium carbonate in the *cog7Δ* strain.

Wild type and *cog7Δ* cells expressing *Candida boidinii* Pmp47 were cultured in SGd medium before switching to HMYO overnight.  All culturing was done at 30ºC.  Oleic acid culture size was 500 mL in a 2 L flask.  Organellar (25,000xg) pellets were extracted with 0.1 M sodium carbonate for 1 hour on ice before spinning at 100,000xg for 30 minutes.  Proteins from equal cell equivalents of each sample were separated by SDS-PAGE, transferred to nitrocellulose, and immunoblotted for Pmp47.  Using the wild type blot as a standard, the *cog7Δ* strain showed increased extractability for the peroxisomal protein, Pmp47.
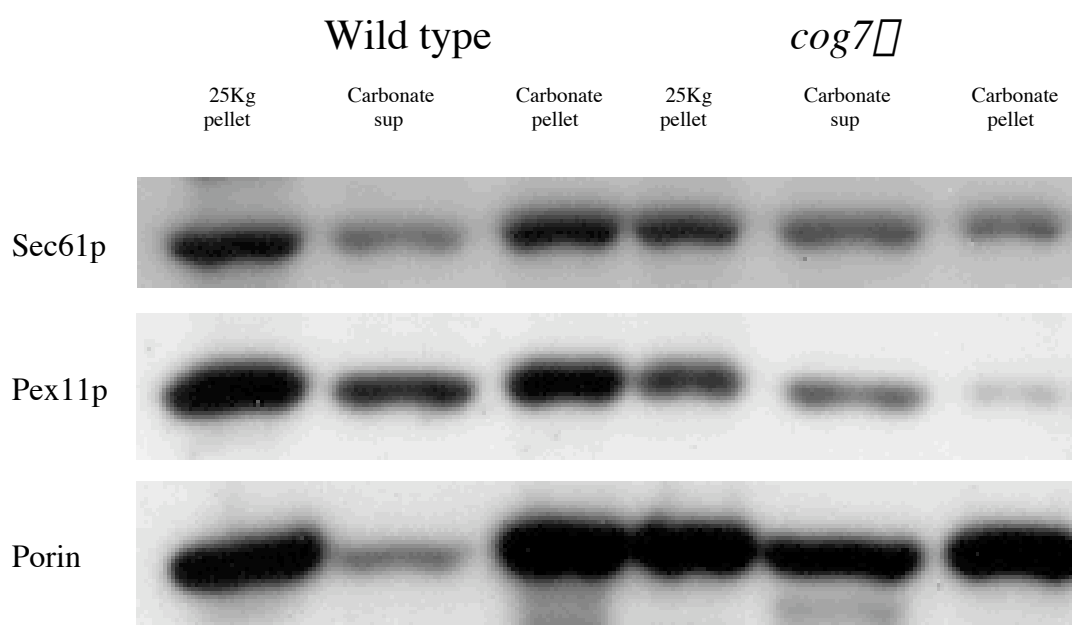
Figure 15    Organellar proteins were more extractable with sodium carbonate in the
            *cog7Δ* strain.

Wild type and *cog7Δ* cells were cultured on HMYO.  Equal protein amounts of organellar
pellets (25,000xg pellets) were extracted with 0.1 M sodium carbonate for 1 hour on ice
before spinning at 100,000xg for 30 minutes.  Proteins from equal cell equivalents of each
sample were separated by SDS-PAGE, transferred to nitrocellulose, and immunoblotted for
the indicated proteins.  Using the wild type blots as standards, the *cog7Δ* strain showed
increased extractability for Pex11p, Sec61p, and porin.  These were markers for peroxisomes,
the ER, and mitochondria, respectively.
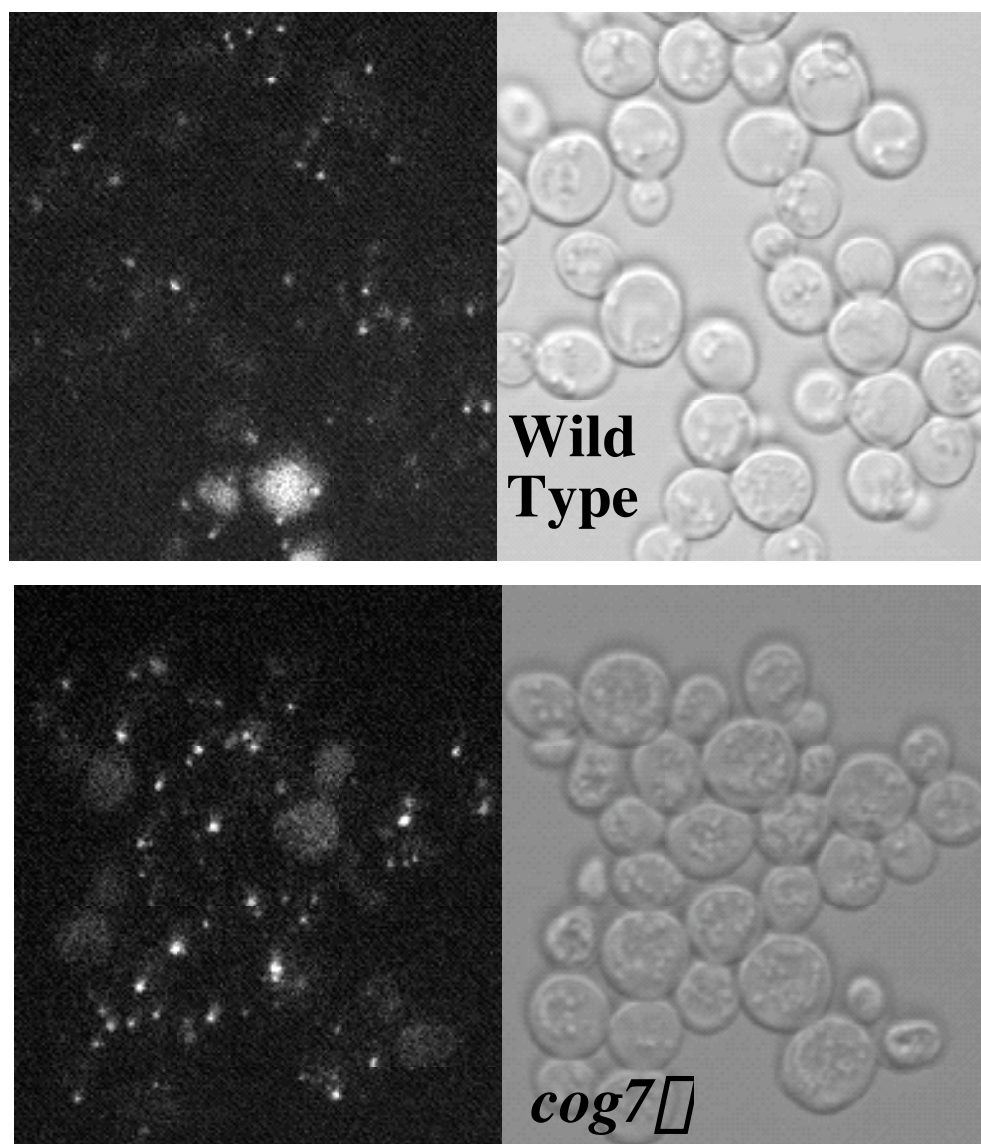
Figure 16        GFP-AKL targeted to punctate organelles in the *cog7Δ* strain.

Clone 10 wild type and *cog7Δ* cells contain a genomic integration of GFP-AKL were grown on SD before visualization.  Both strains showed a punctate pattern that was characteristic of peroxisomal staining.

## PEROXISOME  NUMBERS
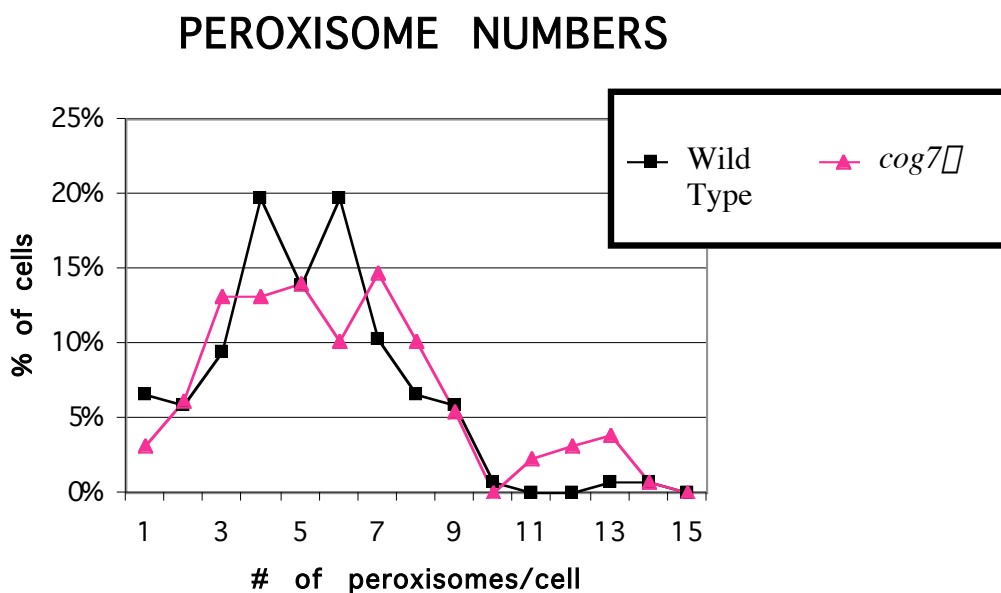


Figure 17    The *cog7Δ* strain contained normal numbers of peroxisomes.

Spontaneous adenine[+] revertants of the Clone 10 strains were obtained by growth on SD medium lacking adenine.  The strains were then cultured in SGd before switching to HMYO. Cells were visualized with a confocal laser scanning microscope to obtain Z series in 0.3 μm increments.  The numbers of individual fluorescent dots per cell were determined.  The peroxisomes in 137 wild type and 129 *cog7Δ* cells were counted.  Data were graphed as the percentage of total number of cells versus the number of peroxisomes per cell.
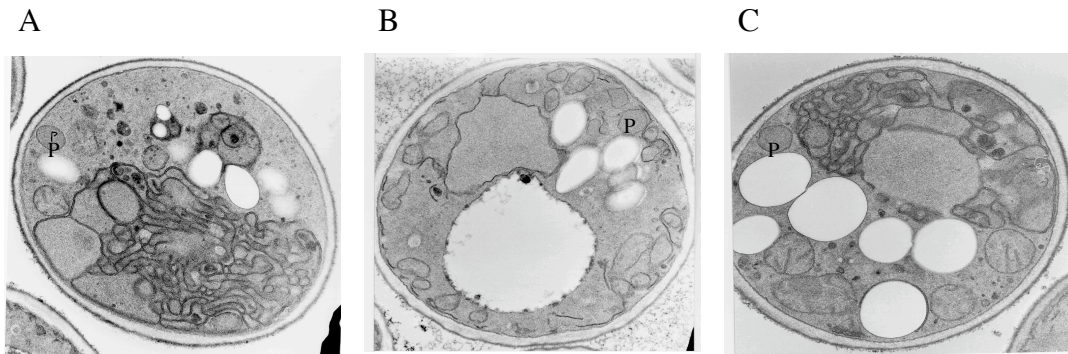
Figure 18     The *cog7Δ* strain displayed distinct peroxisomes and mitochondria, as well as
massive proliferation of internal membranes.

(A) *cog7Δ*  (B) *cog7Δ* complemented and (C) *cog7Δ* mock complemented
cells were grown in HMYO overnight and processed for electron microscopy.  The cells
contained distinguishable peroxisomes (P) and mitochondria.  A and C depict the massive
proliferation of internal membranes.
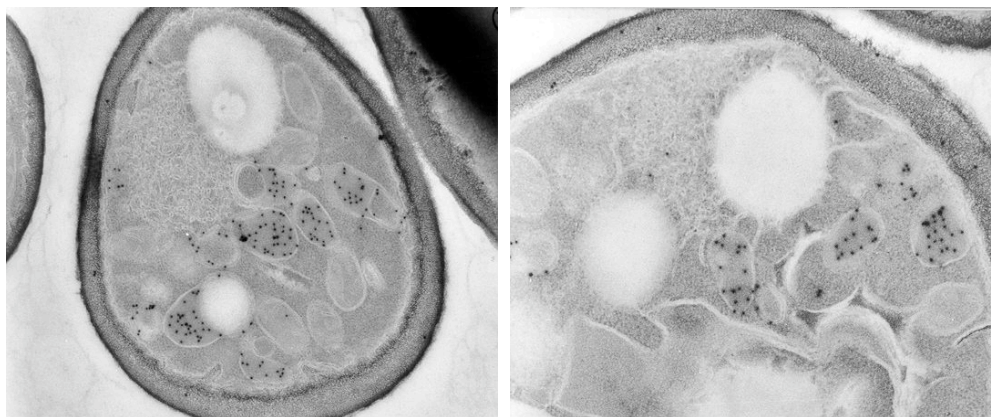
Figure 19        Thiolase targeted to the peroxisomal matrix in the *cog7Δ* strain.


MMYO11α*::cog7Δ* cells were grown in HMYD until they were rapidly dividing before switching them to HMYO.  Cells were processed for immunogold labeling of the peroxisomal matrix protein, thiolase, as described in Materials and Methods.  Shown are two images that also display the proliferation of internal membranes.

Figure 20      The *cog7Δ* strain displayed massive proliferation of the endoplasmic reticulum.

MMYO11α*::cog7Δ* cells were grown in HMYO overnight and processed for electron microscopy.  Arrows indicate where the outer nuclear envelope is proliferating.

Pmp47-(1-267)-GFP                    Thiolase
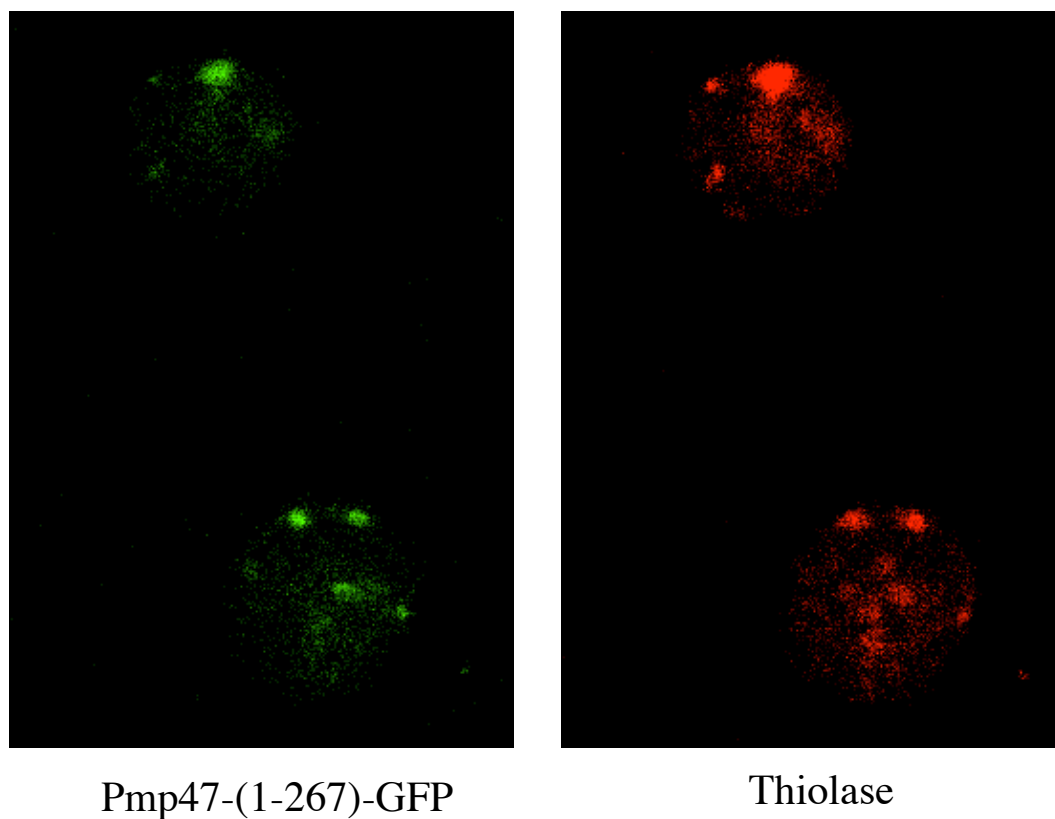
Figure 21        Pmp47-(1-267)-GFP colocalized with thiolase in the *cog7Δ* strain.

MMYO11α*::cog7Δ* cells transformed with pPmp47-(1-267)-GFP were grown in HMYO overnight, fixed, and stained with primary antibodies to thiolase and fluorescently labeled secondary antibodies.  Shown are the fluorescent patterns of GFP and Texas Red conjugated secondary antibodies for two cells.  The Texas Red fluorescence was present everywhere GFP fluorescence was seen.

*Increased amounts of free fatty acid and triolein in the* cog7Δ *strain*

In the course of investigating peroxisomal biogenesis in the *cog7Δ* strain, it was shown that deletion of either *COG7* or *COG8* impaired growth on fatty acid medium. The impaired growth of the *cogΔ* strains signifies that the COG complex is necessary for the proper metabolism of fatty acids. Fatty acids that are imported from the environment are used for a multitude of purposes (DiRusso and Black, 1999; Trotter, 2001).  These include transcriptional control (Rottensteiner et al., 1996; Karpichev et al., 1997), protein modification, and lipid biosynthesis (Oelkers et al., 2000).  Since the break down of fatty acids is normal in the *cog7Δ* strain, the problem must lie with the fatty acids themselves or with their incorporation into more complex species.

Whole cell lipid analysis was done to look for gross differences in the lipid content of *cog7Δ* cells.   There were no differences in neutral and polar lipids in glucose grown mutant cells, but in oleic acid grown *cog7Δ* cells, there was three to four times as much triolein and free oleic acid as in wild type cells (figure 17).  I also analyzed the lipid content of cells grown in the oleic/lauric acids mixture for the wild type, *cog7Δ*, and *pex19Δ* strains.  The amount of free fatty acid, FFA, in the *pex19Δ* strain was higher than that in the wild type strain (figure 18).  This is consistent with a build up of the substrate that cannot be broken down.  The *cog7Δ* strain had higher levels of FFA than both the wild type and *pex19Δ* strains.  These data show that the *cog7Δ* strain accumulates high levels of free fatty acid and the storage lipid triolein to an extent that cannot be explained by the absence of β-oxidation.

The observation of increased amounts of free fatty acid in the cells, offered a possible explanation for the increased extractability of membrane proteins and the aberrant

migration of organelles on density gradients.  These phenotypes could be caused from a high content of free fatty acid in these membranes.  To provide some support for this notion, I attempted to purify peroxisomes from *cog7Δ* cells that had been induced without oleic acid. I created $\rho^0$ (rho zero) wild type and $\rho^0$ *cog7Δ* strains to do this.  Upon loss of mitochondrial DNA, thus creating $\rho^0$ muntants, peroxisomes are induced in raffinose grown cells to compensate for the loss of respiratory function through upregulation of the glyoxylate cycle (Epstein et al., 2001).  The protein patterns of density gradients were the same for the $\rho^0$ wild type and $\rho^0$ *cog7Δ* strains (figure 19), and the extraction of Pex11p was normal in the $\rho^0$ *cog7Δ* strain (figure 20).  The increased extractability and aberrant migration are oleate specific phenotypes, likely caused from the excess intracellular fatty acid.

*Increased rates of fatty acid import in the* cog7Δ *strain*

The simplest interpretation of the above results is that fatty acid uptake in the *cog7Δ* strain is unchecked.  The rate of import out paces that of catabolism causing intracellular fatty acid levels to rise, which in turn, prompts the storage of the excess lipid as triolein.  To address the issue of fatty acid import into *cog7Δ* cells, two experimental approaches were used:  1) measuring the rate of cellular association of $^{14}$C oleic acid and 2) monitoring the intracellular accumulation of a fluorescently labeled fatty acid.  The first approach offers the advantage of using an unmodified fatty acid but does not offer a way to assess transport of the fatty acid across the plasma membrane.  The second approach offers the advantage of visually monitoring the incorporation of the fatty acid into intracellular spaces but utilizes a modified fatty acid.  Together these two approaches should allow

qualitative and quantitative conclusions to be drawn about the import of fatty acids into the

$cog7\Delta$ strain. The specificity of any alterations in the import of fatty acids would be

addressed by measuring the rate of cellular association of $^3$H-glucose. All assays were done

on cells grown to log phase in glucose medium. This was done, in part, to conform to

published techniques, but mostly it was done to reduce the background from dead cells,

which label instantly and intensely with the fluorescent fatty acid.

**Rates of cellular association of $^{14}$C oleic acid.**

Experiments were conducted to determine the linear range of the rate of

cellular association of 10 mM $^{14}$C oleic acid. The rate was linear up to four minutes for both

the wild type and cog7$\Delta$ strains. Figure 21 compares the rates for these two strains

determined using a two-minute incubation time. The rate for the cog7$\Delta$ strain is

approximately two fold greater than the wild type rate.

**Intracellular accumulation of a fluorescently labeled fatty acid.**

The fatty acid probe BODIPY FL C12 (4,4-difluoro-5,7-dimethyl-4-bora-

3a,4a-diaza-s-indacene-3-dodecanoic acid) was used at 10 μM, the same concentration of

fatty acid used to measure the cellular association of $^{14}$C oleic acid. The first experiments

with the probe were done to see if the cog7$\Delta$ strain accumulated more of the probe than wild

type, if the probe labeled intracellular structures, and if any difference in labeling between

the two strains was Cog7p dependent. Figures 22A & B show that the probe did label

intracellular structures in both the cog7$\Delta$ and wild type strains. The label was more intense

for the cog7Δ strain, and the intensity was returned to wild type levels upon reintroduction of *COG7* into the cog7Δ strain.  Figure 22C illustrates that this increased labeling in a cog7Δ strain was not limited to our laboratory strain.  The BY4742*::cog7Δ* strain shows increased accumulation of the fatty acid probe.  To make a tighter connection with this phenotype and the COG complex, the BY4742*::cog8Δ* strain was assayed.  Figure 23 shows that this strain also accumulates the fatty acid probe above wild type levels.

The next experiment with the probe sought to address whether BODIPY FL C12 was an appropriate molecule for monitoring the import of fatty acids.  Assuming that this probe uses the same import pathway as unmodified fatty acids, oleic acid should compete with the probe for import.  To test this, *cog7Δ* cells were incubated with 10 μM probe in the presence of increasing amounts of oleic acid.  Figure 24 shows that the labeling decreases as the amount of oleic acid in the medium increases.  These findings support the notion that results with the probe are indicative of fatty acid import.

Next, we sought to relate this approach to previous experiments showing that the levels of free fatty acids were increased in the *cog7Δ* strain.  The BODIPY FL C12 probe becomes metabolically trapped inside yeast cells after import (Faergeman et al., 2001).  Extensive washing with BSA does not remove the probe from cells (Faergeman et al., 1997; DiRusso et al., 2000).  In an attempt to demonstrate that the probe was in its "free" form and not activated to its CoA ester upon import, *cog7Δ* cells were loaded with the probe and then incubated with fatty acid free bovine serum albumin (BSA).  The assumptions are that the free species would be able to diffuse out of the cells and adsorb onto the BSA while the activated species would remain irreversibly trapped and not diffuse out of the cells.  Figure

25 illustrates that the BSA did reduce the labeling, thereby, suggesting that the probe was in its free form.

**Rates of cellular association of ³H-glucose.**

To address whether the cog7Δ strain was non-specifically importing any molecules from the environment above wild type levels, the cellular association of glucose was monitored. Figure 26 shows that the rates of association are similar for the wild type and cog7Δ strains, suggesting the increased uptake of free fatty acids is a specific phenomenon.

*The Internal pH of* cog7Δ *Cells was Lower than Normal.*

The intracellular pH (pHi) of mammalian cells has been shown to affect the free diffusion of free fatty acids into cells (Trigatti and Gerber, 1996). To demonstrate that this happens in yeast, the import of BODIPY FL C12 was monitored for an *nha1Δ* strain. This strain has a higher pHi than the wild type strain (Sychrova et a., 1999) and would be expected to accumulate more fatty acid by free diffusion. Figure 27 shows that the *nha1Δ* cells did label more intensely than the wild type cells. It is possible, then, that the COG complex regulates the diffusion of free fatty acids across the plasma membrane by regulating the pHi. The intracellular pH of the *cog7Δ* strain, though, was actually lower than that of the wild type strain (figure 28); the *cog7Δ* strain imports more free fatty acid despite having a lower pHi at the time of the onslaught of fatty acids.

Glucose          Oleate

cholesterol ester

triolein

oleic acid

cholesterol

origin

WT | Δ          WT | Δ

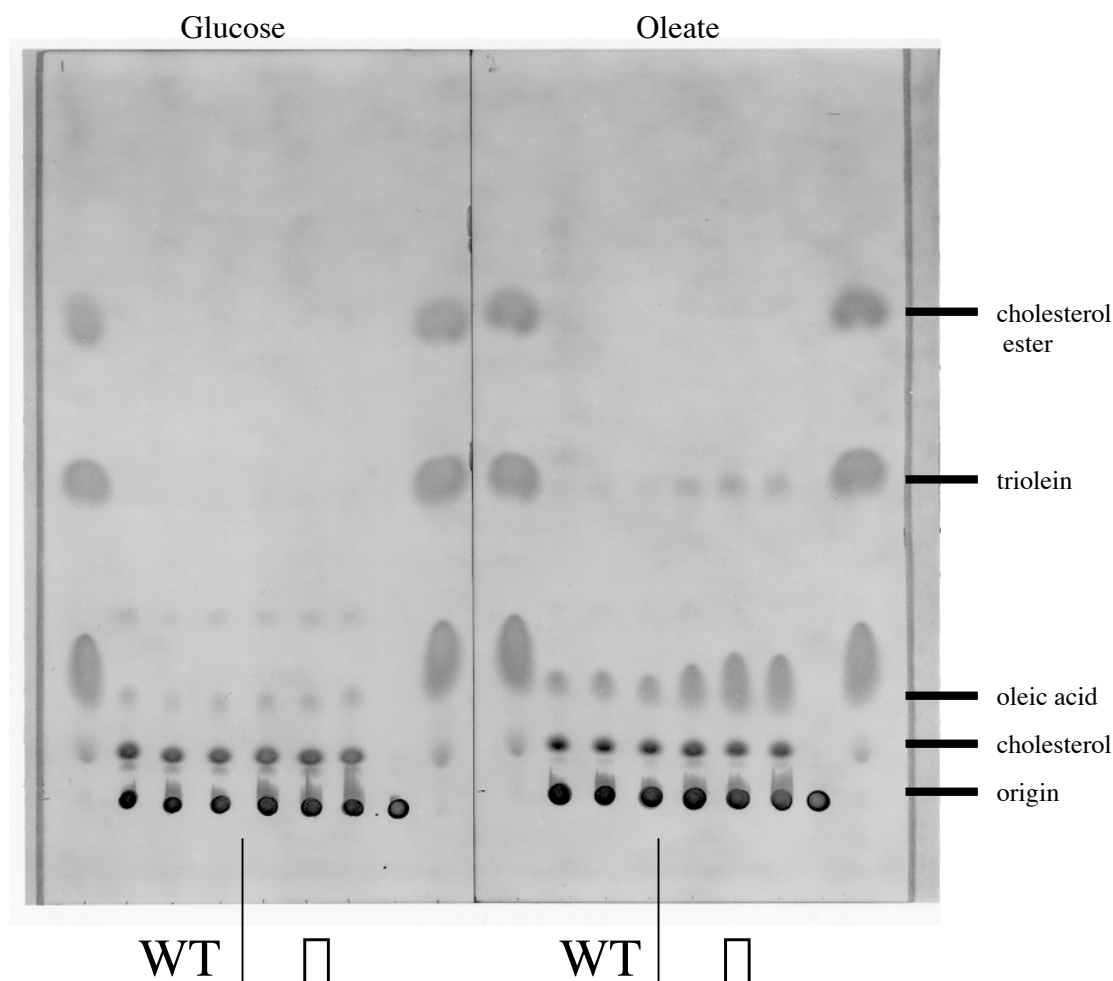Figure 22     The *cog7Δ* strain had a normal lipid profile when grown on glucose, but upon a shift to oleic acid medium, it accumulated high levels of free fatty acid and triolein.

MMYO11α (WT) and MMYO11α::*cog7Δ* (Δ) cells were cultured in either HMYD or HMYO.  Equal optical density units of cells for each strain were extracted in 2-propanol and chloroform.  The organic phase was washed several times with 1M KCl.  The lipids were separated by thin layer chromatography on Si gel G 250 um layer, analytical glass plates.  The solvent was hexane: diethyl ether: acetic acid (80:20:1).  Lipids were visualized with iodine vapor.  Lipid standards are indicated on the right.  The results are shown for three cultures of each strain for each carbon source.
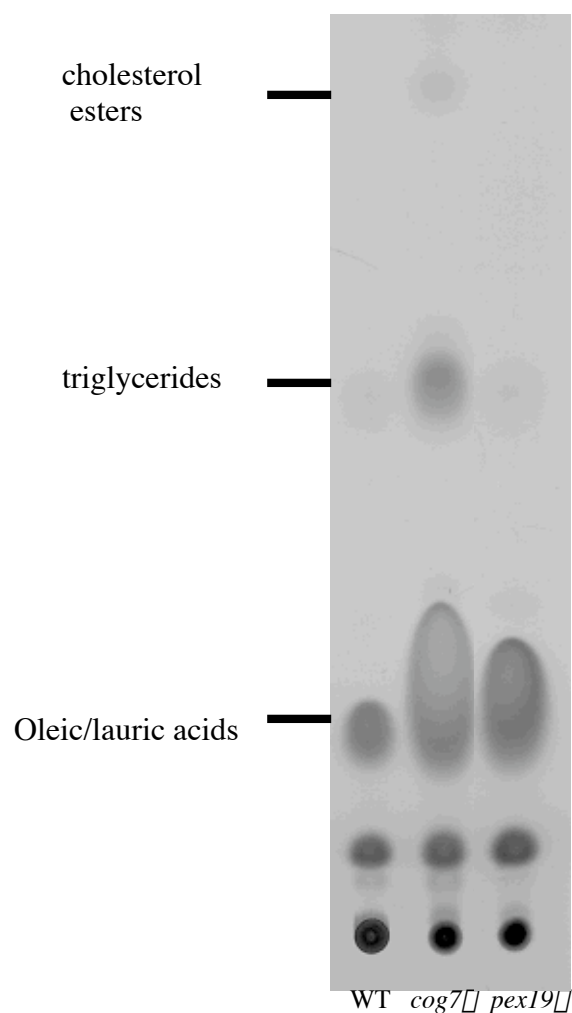
cholesterol esters

triglycerides

Oleic/lauric acids

WT   *cog7Δ*  *pex19Δ*

Figure 23       The *cog7Δ* strain accumulated more free fatty acid and triolein than either the wild type or *pex19Δ* strains.

MMYO11α (WT), MMYO11α::*cog7Δ,* and MMYO11α:: *pex19Δ* were grown on HMYO/L. Equal optical density units of cells for each strain were extracted in 2-propanol and chloroform.  The organic phase was washed several times with 1M KCl.  The lipids were separated by thin layer chromatography on Si gel G 250 um layer, analytical glass plates. The solvent was hexane: diethyl ether: acetic acid (80:20:1).  Lipids were visualized with iodine vapor.  Lipid standards are indicated on the left.
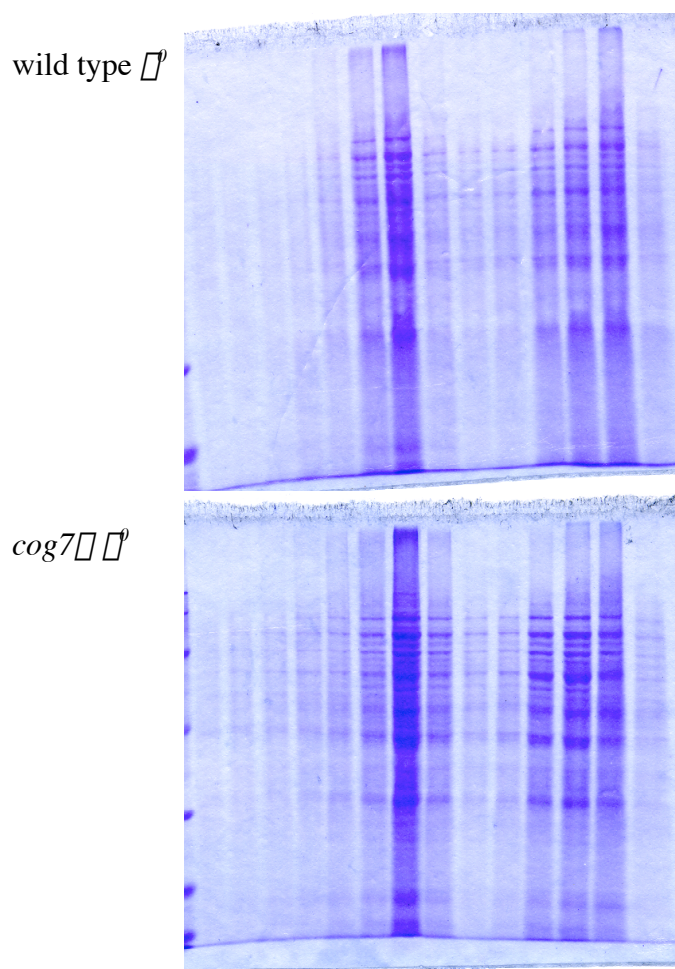
Figure 24     The Nycodenz gradient protein profiles were similar for the wild type $\rho^o$ and $cog7\Delta$ $\rho^o$ strains.

Organelles from wild type $\rho^o$ and $cog7\Delta$ $\rho^o$ were purified according to our standard protocols with the exception of culturing these cells in SR medium (synthetic  2% raffinose).  Shown are the coomassie blue stained SDS-PAGE gels of the Nycodenz fractions.  The protein profiles were similar for both strains.

25,000xg pellet   sup   pellet   25,000xg pellet   sup   pellet

Pex11p

$cog7\Delta\ \rho^o$      Wild Type $\rho^o$

Figure 25    The extraction profiles of Pex11p were similar for the wild type $\rho^o$ and $cog7\Delta$ $\rho^o$ strains.

Organelles from wild type $\rho^o$ and $cog7\Delta$ $\rho^o$ were purified according to our standard protocols with the exception of culturing these cells in SR medium (synthetic 2% raffinose). Shown are the coomassie blue stained SDS-PAGE gels of the Nycodenz fractions. The protein profiles were similar for both strains.
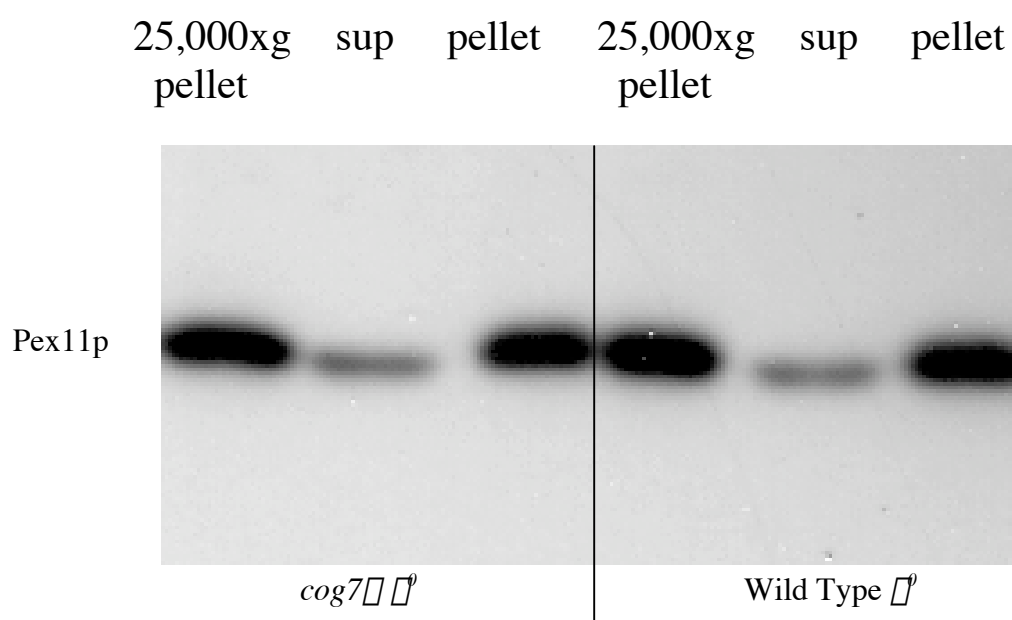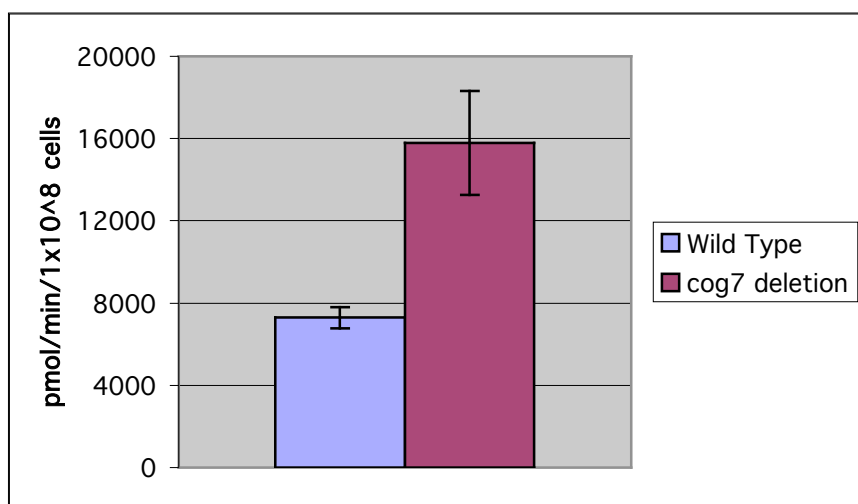
Figure 26      The rate of association of oleic acid was higher for *cog7Δ* cells.

Wild type and *cog7Δ* cells were harvested in log phase from glucose cultures for these assays. Aliquots of cells were incubated with 10 μM $^{14}$C oleic acid for 0 and 2 minutes. Fatty acid free bovine serum albumin (BSA) was added to a final concentration of 25 μM to stop the reactions. Cells were spun down and washed to remove any label not associated with the cells. The amount of cell-associated label was quantified by scintillation counting, and rates for the two minute periods were calculated as pmol/min/1x10^8 cells. Cell counts were determined with a hemacytometer. Shown are the averages +/- SEM for three independent cultures.

A

MMYO11
(wild type)

*cog7Δ*

*cog7Δ*
complemented



B

0 sec          30          60          90



MMYO11
(wild type)

*cog7Δ*

C
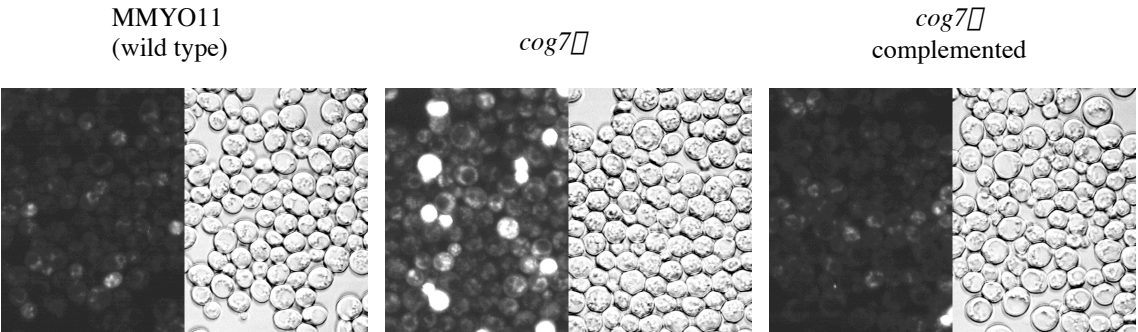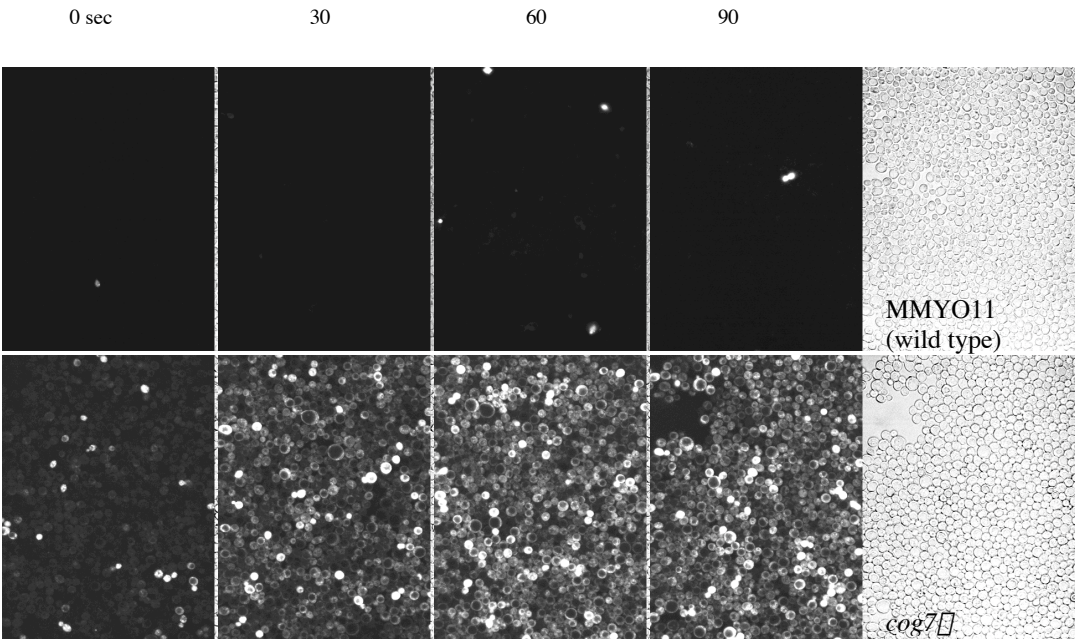


Figure 27    *cog7Δ* cells accumulated higher levels of the fluorescent fatty acid, BODIPY FL C12.

(A) Wild type, *cog7Δ*, and *cog7Δ* complemented cells were harvested in log phase from glucose cultures for these assays.  Aliquots of cells were incubated with 10 μM BODIPY FL C12 (4,4-difluoro-5,7-dimethyl-4-bora-3a,4a-diaza-s-indacene-3-dodecanoic acid) for 10 minutes, washed twice with 50 μM fatty acid free bovine serum albumin (BSA), washed twice with HMS, and viewed with a confocal laser scanning micro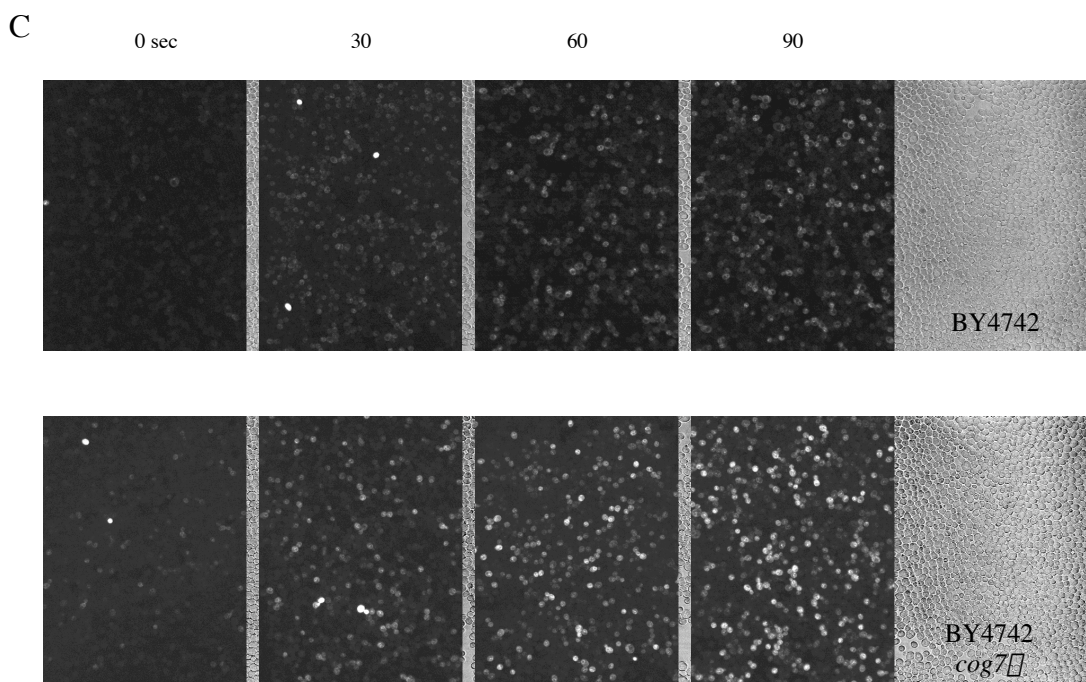scope.  All images were taken with the same settings.  Shown are the fluorescent and corresponding visible fields for each culture.
(B) Wild type and *cog7Δ* cells were harvested in log phase from glucose cultures for these assays.  Aliquots of cells were incubated with 10 μM BODIPY FL C12 for the indicated times.  Reactions were stopped by the addition of fatty acid free BSA to a final concentration of 25 μM, and cells were spun down and washed to remove any probe that was not cell-associated.  All images were taken at the same settings on a confocal laser scanning microscope.  Shown are the fluorescent images of the four time points and the visible fields of the 90 second time points.
(C) BY4742 and BY4742 *cog7Δ* cells were assayed as in (B).

All the images in A-C were taken with the same settings with minor variations in the settings for the visible fields.

BY4742
*cog7Δ*

BY4742
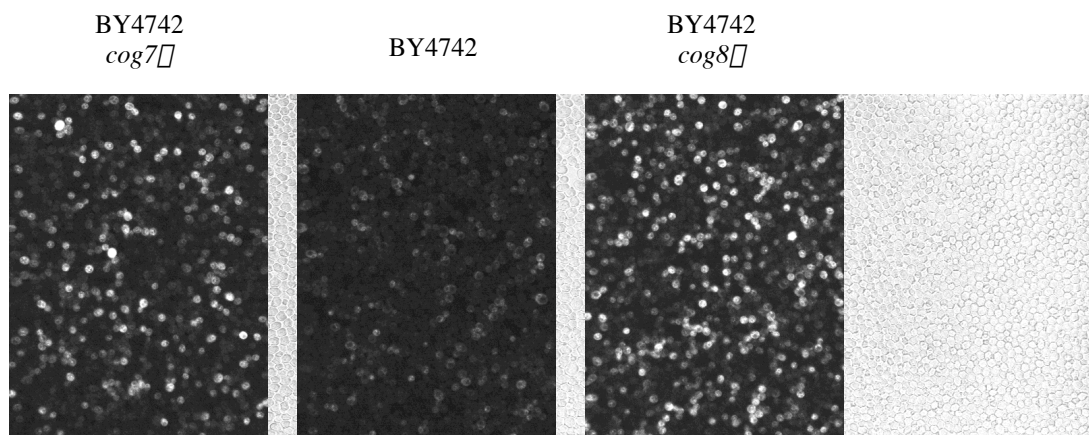
BY4742
*cog8Δ*

Figure 28        Both *cog7Δ* and *cog8Δ* strains accumulated high levels of BODIPY FL C12.

BY4742, BY4742*::cog7Δ,* and BY4742*::cog8Δ* strains were harvested from log phase glucose cultures and incubated with BODIPY FL C12 for 90 seconds.  Fatty acid free BSA was added to 25 µM to stop the reactions, and the cells were washed to remove any free fluorescent fatty acid probe.  Images were taken by confocal laser scanning microscopy.  All images were taken at the same settings.  Shown are the fluorescent images of each strain and the corresponding partial or complete visible fields.

| [BODIPY FL C12] | 10 μM | 10 μM | 10 μM | 10 μM |
| [Oleic acid] | 0 μM | 40 μM | 90 μM | 740 μM |
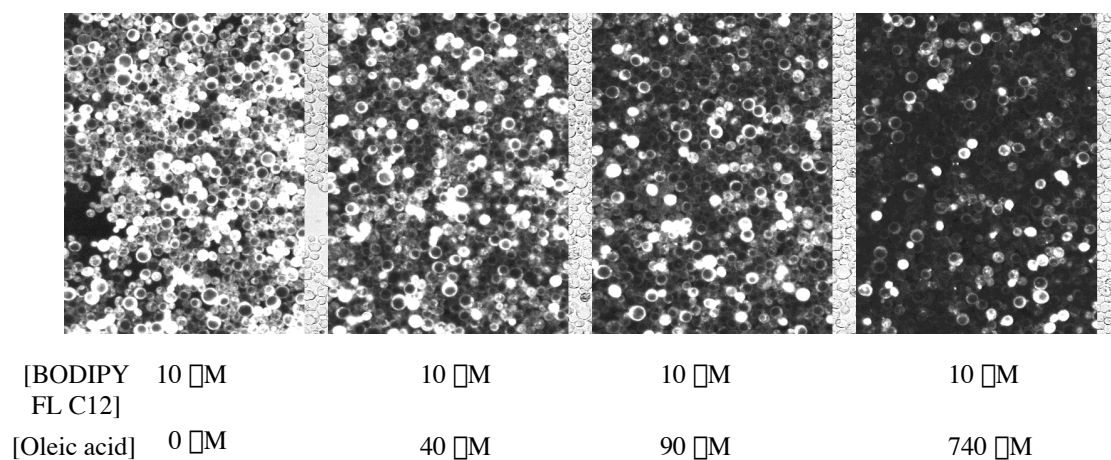
Figure 29     The accumulation of BODIPY FL C12 in *cog7Δ* cells was prevented by co-incubation with oleic acid.

*cog7Δ* cells were harvested in log phase from glucose cultures and treated with 10 μM BODIPY FL C12 with 0, 40, 90, or 740 μM oleic acid for 5 minutes. The cells were washed in HMS and viewed at the same settings on a confocal laser scanning microscope. Shown are the fluorescent images for all oleic acid concentrations and partial images of the visible fields.

A

No BSA | 50 µM BSA for 2 minutes | 50 µM BSA for 15 minutes

B

No BSA | 50 µM BSA for 2 minutes
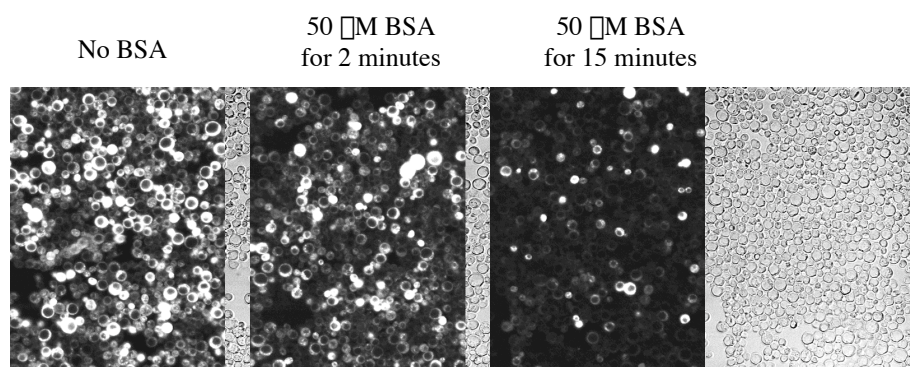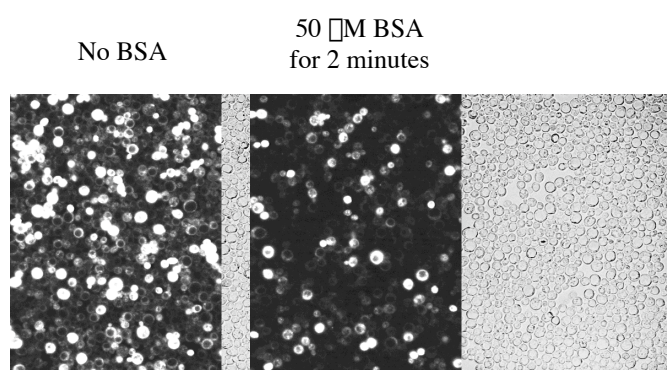
Figure 30    Incubation with fatty acid free bovine serum albumin reversed the accumulation of BODIPY FL C12 in *cog7Δ* cells.

(A)  *cog7Δ* cells were harvested in log phase from glucose cultures and treated with 10 µM BODIPY FL C12 for 5 minutes.  The cells were then treated with no fatty acid free BSA, 50 µM BSA for 2 minutes, or 50 µM BSA for 15 minutes.  The cells were washed, and images were taken by confocal laser scanning microscopy.  All images were taken at the same settings.  Shown are the fluorescent and corresponding visible fields for each treatment.  (B) *cog7Δ* cells were harvested in log phase from glucose cultures and treated with 10 µM BODIPY FL C12 for 90 seconds.  The cells were then treated with no fatty acid free BSA or 50 µM BSA for 2 minutes.  The cells were washed, and images were taken by confocal laser scanning microscopy.  All images were taken at the same settings.  Shown are the fluorescent and corresponding visible fields (partial and complete) for each treatment.
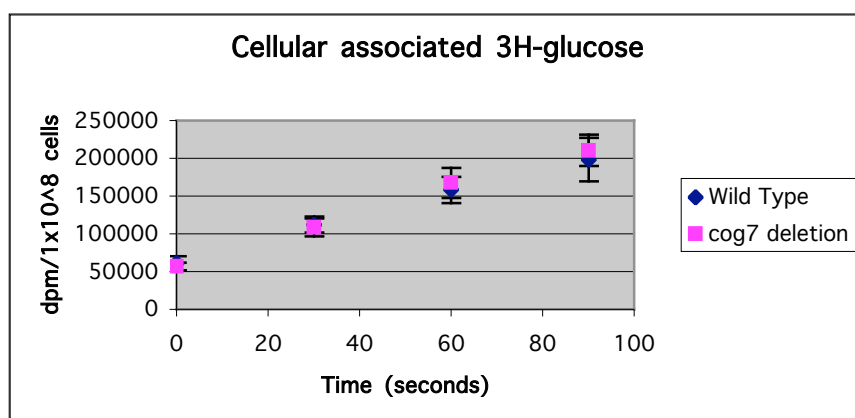
Figure 31     The cellular association of glucose was normal for the *cog7Δ* strain.

Wild type and *cog7Δ* cells were grown to log phase in glucose, starved for 5 hours, and treated with 200 nM $^3$H-glucose.  Aliquots of cells were filtered and washed at 0, 30, 60, and 90 seconds.  The cell-associated (filter-associated) radioactivity was quantified by scintillation counting.  Controls for non-specific binding of glucose to the filters were used, and these background counts were subtracted out.  Shown are the results expressed in disintegrations per minute/1x10^8 cells versus time for the averages +/- the standard deviation of six determinations at each time point for each strain (three determinations each for two independent cultures).
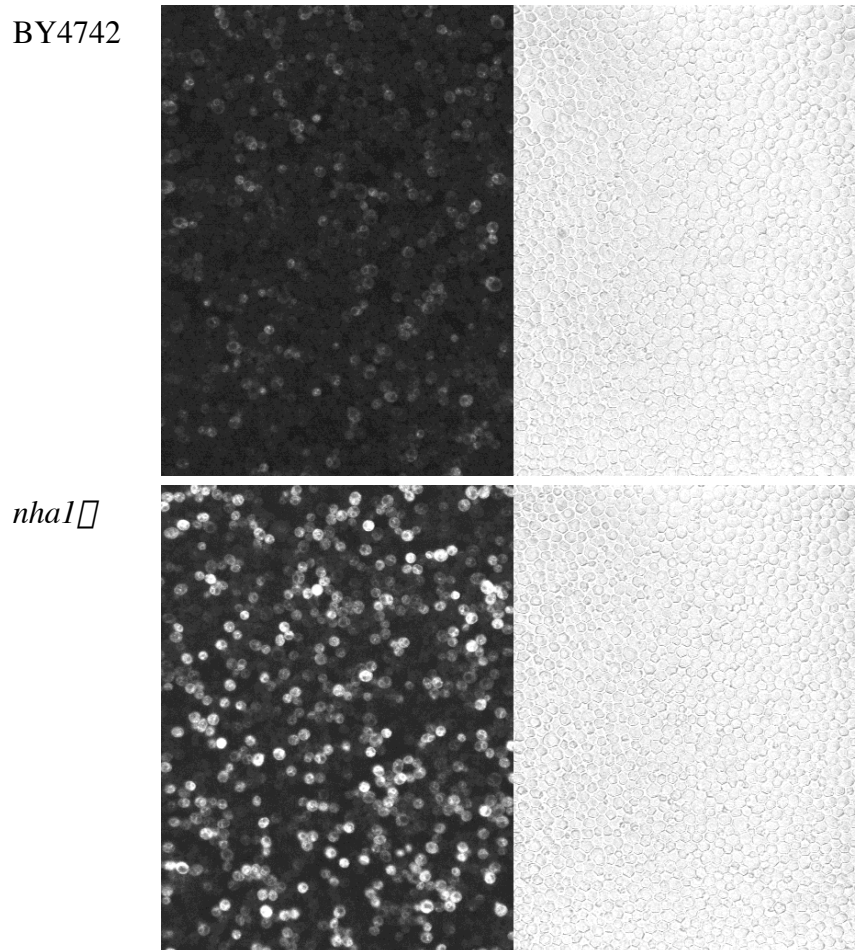
Figure 32      The *nha1Δ* strain accumulated high levels of BODIPY FL C12.

BY4742 and BY4742*::nha1Δ* strains were harvested from log phase glucose cultures and incubated with BODIPY FL C12 for 90 seconds.  Fatty acid free BSA was added to 25 μM to stop the reactions, and the cells were washed to remove any free fluorescent fatty acid probe. Images were taken by confocal laser scanning microscopy.  All images were taken at the same settings.  Shown are the fluorescent images of each strain and the corresponding visible fields.
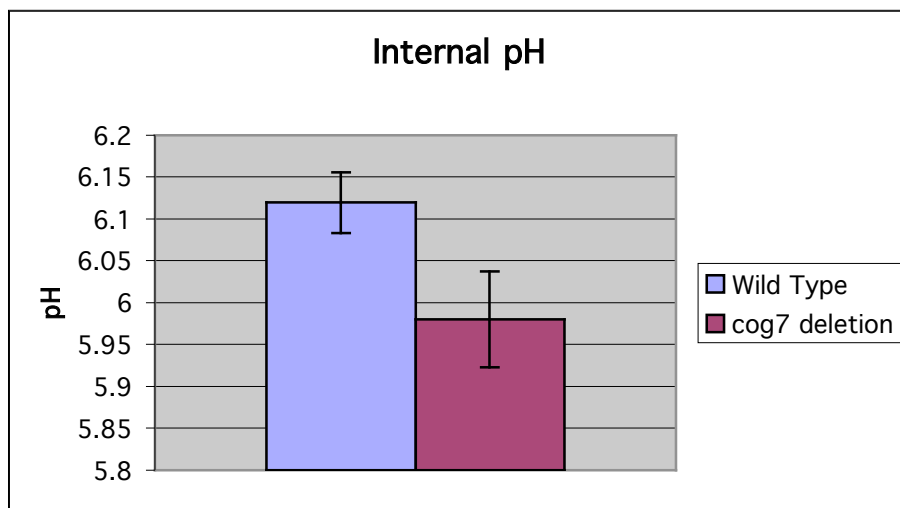
Figure 33    The intracellular pH (pH$_i$) of *cog7Δ* cells was lower than wild type pH$_i$.

The intracellular pH (pH$_i$) was determined for MMYO11α wild type and MMYO11α*::cog7Δ* with the fluorescent dye, pyranine, according to the method outlined by Pena, 1995.  The pH$_i$ was measured after the cells had grown for 48 hrs in SGd.

CONCLUSIONS

Study into the function of Cog7p began as part of a larger effort to elucidate mechanisms of peroxisome biogenesis and function. *COG7* was identified in a two-hybrid screen for proteins that interacted with the mPTS of Pmp47. The goal of my project was to determine if Cog7p was necessary for targeting Pmp47 to peroxisomes. The experimental approach was as follows: 1) determine if *COG7* was an essential gene, 2) if it was not, then create the *cog7Δ* strain so that 3) the state of peroxisomal biogenesis in the absence of Cog7p could be evaluated. I found that the *COG7* gene was not essential. I made the *cog7* deletion strain. I observed no defects in peroxisomal biogenesis in this strain. When Pmp47 was seen in peroxisomes in the *cog7Δ* strain, the call was made that Cog7p was not required for peroxisomal membrane protein targeting.

Interest in Cog7p did not end there, though. In the course of studying the *cog7Δ* strain, it became clear that this protein was needed to properly handle an onslaught of extracellular fatty acids. The *cog7Δ* cells import fatty acids at an abnormally high rate. It seems that the cells try to compensate for the increase by storing more lipid as triolein and, perhaps in some cases, by upregulating the production of ER bilayers. In the end, though, these measures prove inadequate, as the strain grows very poorly on fatty acid medium.

During efforts to determine the subcellular location of Cog7p in an attempt to gain insight into its function, reports came out claiming that it was part of the multiprotein COG complex. I obtained another *cogΔ* strain and subjected it to experiments relating to lipid metabolism. With those results I was convinced to make the second name change for

74

Cog7p—from the generic peroxin designation PexXp given by me to the Cod5p moniker bestowed by Whyte and Munro (2001) and finally to the COG nomenclature proposed by Ungar et al (2002). The burning question then was how did the COG complex regulate the import of fatty acids. The COG complex functions in a pathway that is responsible for the trafficking of many types of proteins and lipids. Although results indicate that the complex operates within the Golgi, effects of its absence resonate throughout the secretory system, from the ER to the plasma membrane. The known and inferred pathways of fatty acid import require plasma membrane proteins. The COG complex, either directly or indirectly, may be required for the maturation of one or more of these proteins (figure 34).

Two mechanisms of fatty acid import have been demonstrated in mammals (Trigatti and Gerber, 1996; Hamilton and Kamp, 1999; Schaffer 2002). One relies solely on passive diffusion through membranes. The protonated form of a fatty acid is thought to flip-flop readily between bilayer leaflets while the charge on the ionized form prevents this species from partitioning. The pH of the aqueous environments adjacent to bilayers can affect the ionization of fatty acids, and thus, their diffusion through membranes. The other mechanism is a protein-mediated process requiring membrane bound fatty acid transport proteins. *E. coli* require a similar facilitated transport mechanism because their hydrophilic envelopes prevent diffusion (DiRusso and Black, 1999). A protein-mediated system has also been characterized in yeast, and a second, uncharacterized mechanism is known to operate (Faergeman et al., 2001). It is thought to involve diffusion, but at this point in time, a role for diffusion is just speculation. Facilitated transport is generally tightly linked with the production of acyl-CoA thioesters in a process called vectorial acylation, but there is one

exception, which I will explore momentarily. Diffusion involves the free fatty acid species. The *cog7Δ* strain accumulates the free species, so I chose to address the issue of how the COG complex regulates fatty acid import using the diffusion model.

The diffusion model predicts that cells with higher intracellular pH values would import more fatty acid. This prediction was borne out in the experiments with the *nha1Δ* strain. Although, this was not definitive proof that the diffusion mechanism operates in *S. cerevisiae,* it was compelling enough to proceed with an investigation into the intracellular pH of the *cog7Δ* strain. The $pH_i$ of the *cog7Δ* strain was actually lower than wild type's. Based on this, I would predict that fatty acid import would be impaired. These experiments, though, were done in the absence of exogenously added fatty acid. This may be important because the lower $pH_i$ of the *cog7Δ* strain suggests that this mutant has trouble with ion homeostasis. It has been demonstrated that diffusion of fatty acids across lipid bilayers can change the pHi of vesicles (Kamp and Hamilton, 1992). The *cog7Δ* strain may not be able to adjust correctly to an influx of protons from flip-flopping fatty acids. The mechanism used to offset this influx may not shut down properly resulting in a higher $pH_i$ and greater influx of fatty acids. I propose that the $pH_i$ at the time of fatty acid addition may not be as important for fatty acid import as is the response by cells to maintain their $pH_i$. Measurements of $pH_i$ before, during, and after fatty acid assaults are needed to evaluate this proposal. If the $pH_i$ measurements warrant, changes in the subcellular localization or modification of ion transporters known to regulate $pH_i$ can be monitored in the *cogΔ* strains.

There is a protein in *S. cerevisiae* that is required for the transport of fatty acids across the plasma membrane. Its role has been clearly defined in relation to fatty acyl-

CoA synthetases, with which Fat1p interacts to constitute a vectorial acylation pathway of

fatty acid import. Reports showed a tight association between the action of Fat1p and the

fatty acyl CoA synthetase, Faa1p (Faergeman et al., 2001; Zou et al., 2002, 2003). Evidence

was also provided of a physical interaction between them. The linkage between Faa1p and

Fat1p was not absolute, as the actions of these two proteins could be uncoupled. Faergeman

et al (1997) demonstrated that upon deletion of *FAT1* the amount of intracellular free fatty

acid was reduced. The report concluded that Fat1p was involved in the transport of free fatty

acids prior to their activation. The implication was that a protein mediated transport system

for free fatty acids existed in *S. cerevisiae*. Additionally, import of fatty acids was not

completely abolished in the *fat1Δ* strain, which was an indication that other pathways for

importing fatty acids existed. It is possible that proper association of the Fat1p complex

requires the action of Cog7p, and that Fat1p function is unregulated in *cogΔ* strains. If this is

true, then the increased accumulation of free fatty acids in the *cog7Δ* strain should be

dependent on the presence of Fat1p. This hypothesis can be tested with an evaluation of the

influx of fatty acids into a *cog7Δ fat1Δ* double deletion strain.

The mechanism of fatty acid import in *S. cerevisiae* can be summed up this

way: there is a Fat1p-dependent process, and there is at least one Fat1p-independent process.

The mechanism at work in the *cogΔ* strains could conceivably fall into either grouping. If it

is the former, then study into the Fat1p complex in *cogΔ* strains should reveal novel aspects

of its regulation, as there are no reports linking increased rates of free fatty acid to Fat1p

function. If it is the latter, then the *cogΔ* strains can be used to define another fatty acid

import pathway in yeast by identifying proteins that are required for the fatty acid

accumulation.  Evaluations of individual double mutants of *cog7* with every non-essential

gene in *S. cerevisiae* might identify such proteins.  There are hurdles involved in creating all

of the double deletions and screening them.  These could be overcome by making random

*cog7* deletions in the deletion set and screening the *cog7Δ geneXΔ* mutants by fluorescence

activated sorting for those that do not accumulate BODIPY FL C12.  The *cogΔ* strains can

serve as valuable tools for the characterization of fatty acid import pathways in *S. cerevisiae*.
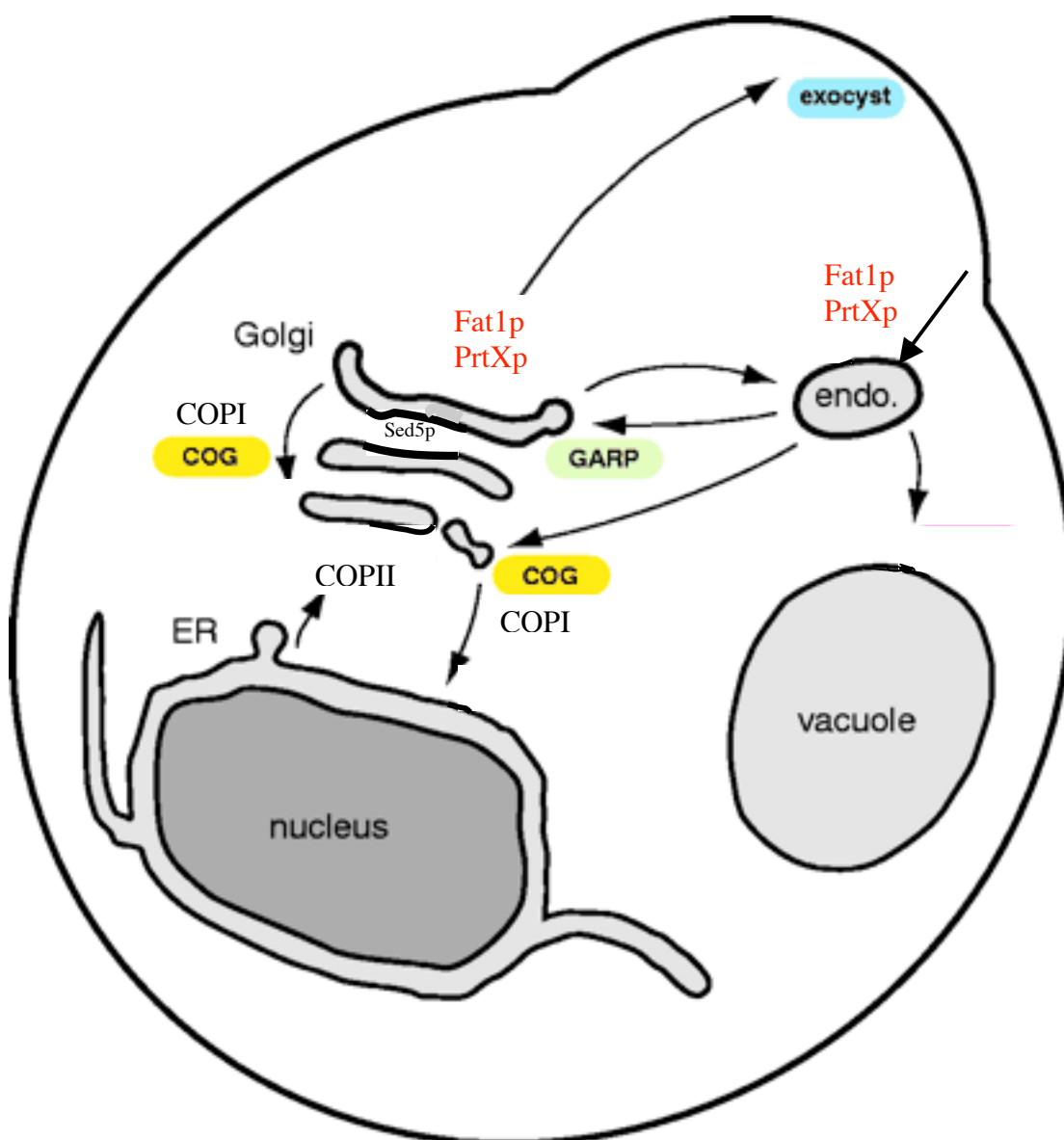
*Adapted from Whyte and Munro, 2002

Figure 34    The maturation or recycling of proteins involved in fatty acid import may
             require the secretory/endocytic pathways.

Fat1p, which controls the import of fatty acids, may traverse the secretory pathway before
taking up residence at the plasma membrane.  Unidentified proteins (PrtXp) that function in a
Fat1p-independent mechanism of import, likewise, might travel through the secretory
system.  The recycling of these proteins may be necessary to regulate their activities by
sequestration or degradation.  The COG complex could be required either directly or
indirectly for the vesicular transport mediating the maturation and recycling of these proteins.

ACKNOWLEDGEMENTS

BIBLIOGRAPHY

Bruinsma P, Spelbrink RG, Nothwehr SF. *Retrograde transport of the mannosyltransferase Och1p to the early Golgi requires a component of the COG transport complex.* **J Biol Chem**. 2004 Jun 30

Conibear E, Cleck JN, Stevens TH. *Vps51p mediates the association of the GARP (Vps52/53/54) complex with the late Golgi t-SNARE Tlg1p.* **Mol Biol Cell**. 2003 Apr;14(4):1610-23.

DiRusso CC, Black PN. *Long-chain fatty acid transport in bacteria and yeast. Paradigms for defining the mechanism underlying this protein-mediated process.* **Mol Cell Biochem**. 1999 Feb;192(1-2):41-52.

Dirusso CC, Connell EJ, Faergeman NJ, Knudsen J, Hansen JK, Black PN. *Murine FATP alleviates growth and biochemical deficiencies of yeast fat1Delta strains.* **Eur J Biochem**. 2000 Jul;267(14):4422-33.

Dyer JM, McNew JA, Goodman JM. *The sorting sequence of the peroxisomal integral membrane protein PMP47 is contained within a short hydrophilic loop.* **J Cell Biol**. 1996 Apr;133(2):269-80.

Epstein CB, Waddle JA, Hale W 4th, Dave V, Thornton J, Macatee TL, Garner HR, Butow RA. *Genome-wide responses to mitochondrial dysfunction.* **Mol Biol Cell**. 2001 Feb;12(2):297-308.

Erdmann R, Veenhuis M, Kunau WH. *Peroxisomes: organelles at the crossroads.* **Trends Cell Biol.** 1997 Oct:7:400-407.

Faergeman NJ, DiRusso CC, Elberger A, Knudsen J, Black PN. *Disruption of the Saccharomyces cerevisiae homologue to the murine fatty acid transport protein impairs uptake and growth on long-chain fatty acids.* **J Biol Chem**. 1997 Mar 28;272(13):8531-8.

Faergeman NJ, Black PN, Zhao XD, Knudsen J, DiRusso CC. *The Acyl-CoA synthetases encoded within FAA1 and FAA4 in Saccharomyces cerevisiae function as components of the fatty acid transport system linking import, activation, and intracellular utilization.* **J Biol Chem**. 2001 Oct 5;276(40):37051-9.

Fang Y, Morrell JC, Jones JM, Gould SJ. *PEX3 functions as a PEX19 docking factor in the import of class I peroxisomal membrane proteins.* **J Cell Biol**. 2004 Mar 15;164(6):863-75.

Farkas RM, Giansanti MG, Gatti M, Fuller MT. *The Drosophila Cog5 homologue is required for cytokinesis, cell elongation, and assembly of specialized Golgi architecture during spermatogenesis.* **Mol Biol Cell**. 2003 Jan;14(1):190-200.

Fox TD, Folley LS, Mulero JJ, McMullin TW, Thorsness PE, Hedin LO, Costanzo MC. *Analysis and manipulation of yeast mitochondrial genes.* **Methods Enzymol**. 1991;194:149-65.

Geuze HJ, Murk JL, Stroobants AK, Griffith JM, Kleijmeer MJ, Koster AJ, Verkleij AJ, Distel B, Tabak HF. *Involvement of the endoplasmic reticulum in peroxisome formation.* **Mol Biol Cell**. 2003 Jul;14(7):2900-7. Epub 2003 Apr 04.

Gibson TJ. *Studies on the Epstein-Barr virus genome*. **Ph.D. thesis** 1984 Cambridge University, England.

Girzalsky W, Rehling P, Stein K, Kipper J, Blank L, Kunau WH, Erdmann R. *Involvement of Pex13p in Pex14p localization and peroxisomal targeting signal 2-dependent protein import into peroxisomes.* **J Cell Biol**. 1999 Mar 22;144(6):1151-62.

Goodman JM, Maher J, Silver PA, Pacifico A, Sanders D. *The membrane proteins of the methanol-induced peroxisome of Candida boidinii Initial characterization and generation of monoclonal antibodies.* **J Biol Chem**. 1986 Mar 5;261(7):3464-8.

Gotte K, Girzalsky W, Linkert M, Baumgart E, Kammerer S, Kunau WH, Erdmann R. *Pex19p, a farnesylated protein essential for peroxisome biogenesis.* **Mol Cell Biol**. 1998 Jan;18(1):616-28.

Gurvitz A, Mursula AM, Yagi AI, Hartig A, Ruis H, Rottensteiner H, Hiltunen JK. *Alternatives to the isomerase-dependent pathway for the beta-oxidation of oleic acid are dispensable in Saccharomyces cerevisiae. Identification of YOR180c/DCI1 encoding peroxisomal delta(3,5)-delta(2,4)-dienoyl-CoA isomerase.* **J Biol Chem**. 1999 Aug 27;274(35):24514-21.

Hamilton JA, Kamp F. *How are free fatty acids transported in membranes? Is it by proteins or by free diffusion through the lipids?* **Diabetes**. 1999 Dec;48(12):2255-69.

Hettema EH, van Roermund CW, Distel B, van den Berg M, Vilela C, Rodrigues-Pousada C, Wanders RJ, Tabak HF. *The ABC transporter proteins Pat1 and Pat2 are required for import of long-chain fatty acids into peroxisomes of Saccharomyces cerevisiae.* **EMBO J**. 1996 Aug 1;15(15):3813-22.

Hettema EH, Girzalsky W, van Den Berg M, Erdmann R, Distel B. *Saccharomyces cerevisiae pex3p and pex19p are required for proper localization and stability of peroxisomal membrane proteins.* **EMBO J**. 2000 Jan 17;19(2):223-33.

Hsu SC, Ting AE, Hazuka CD, Davanger S, Kenny JW, Kee Y, Scheller RH. *The mammalian brain rsec6/8 complex.* **Neuron**. 1996 Dec;17(6):1209-19.

Imanaka T, Shiina Y, Takano T, Hashimoto T, Osumi T. *Insertion of the 70-kDa peroxisomal membrane protein into peroxisomal membranes in vivo and in vitro.* **J Biol Chem**. 1996 Feb 16;271(7):3706-13.

Ito H, Fukuda Y, Murata K, Kimura A. *Transformation of intact yeast cells treated with alkali cations.* **J Bacteriol**. 1983 Jan;153(1):163-8.

Jones JM, Morrell JC, Gould SJ. *PEX19 is a predominantly cytosolic chaperone and import receptor for class 1 peroxisomal membrane proteins.* **J Cell Biol**. 2004 Jan 5;164(1):57-67.

Kamp F, Hamilton JA. *pH gradients across phospholipid membranes caused by fast flip-flop of un-ionized fatty acids.* **Proc Natl Acad Sci U S A**. 1992 Dec 1;89(23):11367-70.

Karpichev IV, Luo Y, Marians RC, Small GM. *A complex containing two transcription factors regulates peroxisome proliferation and the coordinate induction of beta-oxidation enzymes in Saccharomyces cerevisiae.* **Mol Cell Biol**. 1997 Jan;17(1):69-80.

Kim DW, Sacher M, Scarpa A, Quinn AM, Ferro-Novick S. *High-copy suppressor analysis reveals a physical interaction between Sec34p and Sec35p, a protein implicated in vesicle docking*. **Mol Biol Cell**. 1999 Oct;10(10):3317-29.

Kim DW, Massey T, Sacher M, Pypaert M, Ferro-Novick S. *Sgf1p, a new component of the Sec34p/Sec35p complex*. **Traffic**. 2001 Nov;2(11):820-30.

Laemmli UK. *Cleavage of structural proteins during the assembly of the head of bacteriophage T4*. **Nature**. 1970 Aug 15;227(259):680-5.

Loh E, Hong W. *Sec34 is implicated in traffic from the endoplasmic reticulum to the Golgi and exists in a complex with GTC-90 and ldlBp*. **J Biol Chem**. 2002 Jun 14;277(24):21955-61.

Loh E, Hong W. *The binary interacting network of the conserved oligomeric Golgi tethering complex*. **J Biol Chem**. 2004 Jun 4;279(23):24640-8.

Marshall PA, Krimkevich YI, Lark RH, Dyer JM, Veenhuis M, Goodman JM. *Pmp27 promotes peroxisomal proliferation*. **J Cell Biol**. 1995 Apr;129(2):345-55.

Matsuzono Y, Kinoshita N, Tamura S, Shimozawa N, Hamasaki M, Ghaedi K, Wanders RJ, Suzuki Y, Kondo N, Fujiki Y. *Human PEX19: cDNA cloning by functional*

*complementation, mutation analysis in a patient with Zellweger syndrome, and potential role in peroxisomal membrane assembly.* **Proc Natl Acad Sci U S A**. 1999 Mar 2;96(5):2116-21.

[a]McCammon MT, Veenhuis M, Trapp SB, Goodman JM. *Association of glyoxylate and beta-oxidation enzymes with peroxisomes of Saccharomyces cerevisiae.* **J Bacteriol**. 1990 Oct;172(10):5816-27.

[b]McCammon MT, Dowds CA, Orth K, Moomaw CR, Slaughter CA, Goodman JM. *Sorting of peroxisomal membrane protein PMP47 from Candida boidinii into peroxisomal membranes of Saccharomyces cerevisiae.* **J Biol Chem**. 1990 Nov 25;265(33):20098-105.

McCammon MT, McNew JA, Willy PJ, Goodman JM. *An internal region of the peroxisomal membrane protein PMP47 is essential for sorting to peroxisomes.* **J Cell Biol**. 1994 Mar;124(6):915-25.

Morsomme P, Riezman H. *The Rab GTPase Ypt1p and tethering factors couple protein sorting at the ER to vesicle targeting to the Golgi apparatus.* **Dev Cell**. 2002 Mar;2(3):307-17.

Nakagawa T, Imanaka T, Morita M, Ishiguro K, Yurimoto H, Yamashita A, Kato N, Sakai Y. *Peroxisomal membrane protein Pmp47 is essential in the metabolism of middle-chain*

*fatty acid in yeast peroxisomes and Is associated with peroxisome proliferation.* **J Biol Chem**. 2000 Feb 4;275(5):3455-61.

Oelkers P, Tinkelenberg A, Erdeniz N, Cromley D, Billheimer JT, Sturley SL. *A lecithin cholesterol acyltransferase-like gene mediates diacylglycerol esterification in yeast.* **J Biol Chem**. 2000 May 26;275(21):15609-12.

Oka T, Ungar D, Hughson FM, Krieger M. *The COG and COPI complexes interact to control the abundance of GEARs, a subset of Golgi integral membrane proteins.* **Mol Biol Cell**. 2004 May;15(5):2423-35.

Pena A, Ramirez J, Rosas G, Calahorra M. *Proton pumping and the internal pH of yeast cells, measured with pyranine introduced by electroporation.* **J Bacteriol**. 1995 Feb;177(4):1017-22.

Ram RJ, Li B, Kaiser CA. *Identification of Sec36p, Sec37p, and Sec38p: components of yeast complex that contains Sec34p and Sec35p.* **Mol Biol Cell**. 2002 May;13(5):1484-500.

Rottensteiner H, Kal AJ, Filipits M, Binder M, Hamilton B, Tabak HF, Ruis H. *Pip2p: a transcriptional regulator of peroxisome proliferation in the yeast Saccharomyces cerevisiae.* **EMBO J**. 1996 Jun 17;15(12):2924-34.

Sacksteder KA, Jones JM, South ST, Li X, Liu Y, Gould SJ. *PEX19 binds multiple peroxisomal membrane proteins, is predominantly cytoplasmic, and is required for peroxisome membrane synthesis.* **J Cell Biol**. 2000 Mar 6;148(5):931-44.

Sambrook J, Fritsch EF, Maniatis T. *Molecular Cloning: A Laboratory Manual.* 1989 **Cold Spring Harbor Laboratory** Cold Spring Harbor, NY.

Schaffer JE. *Fatty acid transport: the roads taken.* **Am J Physiol Endocrinol Metab**. 2002 Feb;282(2):E239-46.

Schaffner W, Weissmann C. *A rapid, sensitive, and specific method for the determination of protein in dilute solution.* **Anal Biochem**. 1973 Dec;56(2):502-14.

Shani N, Valle D. *A Saccharomyces cerevisiae homolog of the human adrenoleukodystrophy transporter is a heterodimer of two half ATP-binding cassette transporters.* **Proc Natl Acad Sci U S A**. 1996 Oct 15;93(21):11901-6.

Short B, Barr FA. *Membrane traffic: exocyst III--makes a family.* **Curr Biol**. 2002 Jan 8;12(1):R18-20.

Sikorski RS, Hieter P.  *A system of shuttle vectors and yeast host strains designed for efficient manipulation of DNA in Saccharomyces cerevisiae.*  **Genetics**. 1989 May;122(1):19-27.

Smith DB, Johnson KS.  *Single-step purification of polypeptides expressed in Escherichia coli as fusions with glutathione S-transferase.*  **Gene**. 1988 Jul 15;67(1):31-40.

Studier FW, Moffatt BA.  *Use of bacteriophage T7 RNA polymerase to direct selective high-level expression of cloned genes.*  **J Mol Biol**. 1986 May 5;189(1):113-30.

Subramani S.  *Components involved in peroxisome import, biogenesis, proliferation, turnover, and movement.*  **Physiol Rev**. 1998 Jan;78(1):171-88.

Suvorova ES, Duden R, Lupashin VV.  *The Sec34/Sec35p complex, a Ypt1p effector required for retrograde intra-Golgi trafficking, interacts with Golgi SNAREs and COPI vesicle coat proteins.*  **J Cell Biol**. 2002 May 13;157(4):631-43.

Suvorova ES, Kurten RC, Lupashin VV.  *Identification of a human orthologue of Sec34p as a component of the cis-Golgi vesicle tethering machinery.*  **J Biol Chem**. 2001 Jun 22;276(25):22810-8.

Sychrova H, Ramirez J, Pena A. *Involvement of Nha1 antiporter in regulation of intracellular pH in Saccharomyces cerevisiae.* **FEMS Microbiol Lett**. 1999 Feb 15;171(2):167-72.

Tabak HF, Braakman I, Distel B. *Peroxisomes: simple in function but complex in maintenance.* **Trends Cell Biol**. 1999 Nov;9(11):447-53.

Tabak HF, Murk JL, Braakman I, Geuze HJ. *Peroxisomes start their life in the endoplasmic reticulum.* **Traffic**. 2003 Aug;4(8):512-8.

Titorenko VI, Rachubinski RA. *Mutants of the yeast Yarrowia lipolytica defective in protein exit from the endoplasmic reticulum are also defective in peroxisome biogenesis.* **Mol Cell Biol**. 1998 May;18(5):2789-803.

Trigatti BL, Gerber GE. *The effect of intracellular pH on long-chain fatty acid uptake in 3T3-L1 adipocytes: evidence that uptake involves the passive diffusion of protonated long-chain fatty acids across the plasma membrane.* **Biochem J**. 1996 Jan 15;313 ( Pt 2):487-94.

Trotter PJ. *The genetics of fatty acid metabolism in Saccharomyces cerevisiae.* **Annu Rev Nutr**. 2001;21:97-119.

Ungar D, Oka T, Brittle EE, Vasile E, Lupashin VV, Chatterton JE, Heuser JE, Krieger M, Waters MG. *Characterization of a mammalian Golgi-localized protein complex, COG, that is required for normal Golgi morphology and function.* **J Cell Biol**. 2002 Apr 29;157(3):405-15.

van den Bosch H, Schutgens RB, Wanders RJ, Tager JM. *Biochemistry of peroxisomes.* **Annu Rev Biochem**. 1992;61:157-97.

van Roermund CW, Tabak HF, van Den Berg M, Wanders RJ, Hettema EH. *Pex11p plays a primary role in medium-chain fatty acid oxidation, a process that affects peroxisome number and size in Saccharomyces cerevisiae.* **J Cell Biol**. 2000 Aug 7;150(3):489-98.

van Roermund CW, Drissen R, van Den Berg M, Ijlst L, Hettema EH, Tabak HF, Waterham HR, Wanders RJ. *Identification of a peroxisomal ATP carrier required for medium-chain fatty acid beta-oxidation and normal peroxisome proliferation in Saccharomyces cerevisiae.* **Mol Cell Biol**. 2001 Jul;21(13):4321-9.

VanRheenen SM, Cao X, Lupashin VV, Barlowe C, Waters MG. *Sec35p, a novel peripheral membrane protein, is required for ER to Golgi vesicle docking.* **J Cell Biol**. 1998 Jun 1;141(5):1107-19.

VanRheenen SM, Cao X, Sapperstein SK, Chiang EC, Lupashin VV, Barlowe C,Waters MG. *Sec34p, a protein required for vesicle tethering to the yeast Golgi apparatus, is in a complex with Sec35p.* **J Cell Biol**. 1999 Nov 15;147(4):729-42.

Veenhuis M, Mateblowski M, Kunau WH, Harder W. *Proliferation of microbodies in Saccharomyces cerevisiae.* **Yeast**. 1987 Jun;3(2):77-84.

Wang X, Unruh MJ, Goodman JM. *Discrete targeting signals direct Pmp47 to oleate-induced peroxisomes in Saccharomyces cerevisiae.* **J Biol Chem**. 2001 Apr 6;276(14):10897-905.

Watkins PA, Lu JF, Steinberg SJ, Gould SJ, Smith KD, Braiterman LT. *Disruption of the Saccharomyces cerevisiae FAT1 gene decreases very long-chain fatty acyl-CoA synthetase activity and elevates intracellular very long-chain fatty acid concentrations.* **J Biol Chem**. 1998 Jul 17;273(29):18210-9.

Whyte JR, Munro S. *The Sec34/35 Golgi transport complex is related to the exocyst, defining a family of complexes involved in multiple steps of membrane traffic.* **Dev Cell**. 2001 Oct;1(4):527-37.

Whyte JR, Munro S. *Vesicle tethering complexes in membrane traffic.* **J Cell Sci**. 2002 Jul 1;115(Pt 13):2627-37.

Wu X, Steet RA, Bohorov O, Bakker J, Newell J, Krieger M, Spaapen L, Kornfeld S, Freeze HH. *Mutation of the COG complex subunit gene COG7 causes a lethal congenital disorder*. **Nat Med**. 2004 May;10(5):518-23.


Zou Z, DiRusso CC, Ctrnacta V, Black PN. *Fatty acid transport in Saccharomyces cerevisiae. Directed mutagenesis of FAT1 distinguishes the biochemical activities associated with Fat1p*. **J Biol Chem**. 2002 Aug 23;277(34):31062-71.


Zou Z, Tong F, Faergeman NJ, Borsting C, Black PN, DiRusso CC. *Vectorial acylation in Saccharomyces cerevisiae. Fat1p and fatty acyl-CoA synthetase are interacting components of a fatty acid import complex*. **J Biol Chem**. 2003 May 2;278(18):16414-22.

VITA

Johnathan Luke Ballard was born in Bryan, Texas, on November 3, 1973, the son of Mark Ballard and Valerie Ballard.  He graduated as valedictorian of his class at Franklin High School, Franklin, Texas in 1992.  He entered Texas A&M University at College Station, Texas, in September 1992.  He received the degree of Bachelor of Science with a major in genetics from Texas A&M University in May 1996.  In August 1996, he married Karla Lynn Blackmon from Hearne, Texas.  Later that month, he entered the Graduate School of Biomedical Sciences at the University of Texas Southwestern Medical Center at Dallas.  In February1999, his first daughter, Morgan Deane, was born.  In December 2002, he joined the laboratory of Yiwei Jiang, Ph.D. at the Texas A&M University Health Science Center at College Station, Texas.  His second daughter, Kristen Isabelle, was born in August 2003.  He received his Doctor of Philosophy from the University of Texas Southwestern in August 2004.


Permanent Address:　　10480 Woodview Drive
　　　　　　　　　　　College Station, Texas  77845